Nanostructured lipid systems containing waste material of propolis for wound healing: formulation and biological evaluation

Hélen Cássia Rosseto[a], Lucas de Alcântara Sica de Toledo[a], Elisabetta Esposito[b], Giuseppe Valacchi[b], Rita Cortesi[b], Marcos Luciano Bruschi[a]*

[a] Postgraduate Program in Pharmaceutical Sciences, Laboratory of Research and Development of Drug Delivery Systems, Department of Pharmacy, State University of Maringá, Maringá, Paraná, Brazil

[b] Department of Life Sciences and Biotechnology, University of Ferrara, Ferrara, Italy

* Corresponding author.

E-mail address: mlbruschi@uem.br (M.L. Bruschi).

ABSTRACT

Propolis, a natural compound that may help on the acceleration of the wound healing process, is mainly used as ethanolic extract. The extractive solution may also be obtained from the propolis byproduct (BP), transforming this waste material into a pharmaceutical active ingredient. Even if propolis does not present toxicity, when used as an extract over harmed skin or mucosa, the present ethanol content may be harmful to the tissue recovering, besides hindering the drug release.

The present study describes the development of solid lipid nanoparticles (SLN) and nanostructured lipid carriers (NLC) as topic propolis delivery systems, the evaluation of their physicochemical properties, and the healing potential of these preparations.

The extracts were evaluated to guarantee the quality and the lipid dispersions were characterized as morphology (cryo-TEM), size analysis (PCS) and diffractometric (X-ray) characteristics. The occlusive capacity of formulations was also evaluated by the *in vitro* technique, which determines the occlusion factor. The drug entrapment efficiency (EE), as well as the *in vitro* drug release profile from the nanoparticulate systems were investigated as well.

This study allowed the development of lipid nanostrucutures containing complex active agents from propolis. The size analysis performed through 90 days was favorable to a topic administration and the polydispersity index, though not ideal in all cases, due to the high content of resins and gums from the extracts, were relatively stable for the SLN. The propolis extract contributes to the occlusive potential of the formulations. Both extracts (propolis and byproduct) showed good cell viability freely or entrapped on the systems. Finally, it was possible to show that the loaded SLN provided and acceleration of the wound healing process tested *in vivo*.

KEYWORDS: nanotechnology; materials science; formulation; propolis byproduct; nanoparticles; nanostructured lipid carriers.

1. Introduction

Propolis (PRP) or bee glue has many pharmaceutical properties (e.g. antimicrobial, fungicidal, antiviral, immunostimulating, cytostatic, antiulcer, hypotensive, anti-inflammatory and antioxidant) and is used on the wound healing on therapeutics [1-5]. This natural compound is a complex mixture, constituted mainly by resin, waxes, water, inorganics, essential oils, phenolics, and balsamic substances, collected by bees (*Apis mellifera* L.) from flowers, pollen, tree buds, branches and exudates. The collected bulk materials are partially digested by the salivary enzymes of the bees, especially the 13-glucosidase, and regurgitated producing PRP [2,3,6].

Ethanolic extractive solution of PRP is the main dosage form utilized on therapeutics. After the preparation of the PRP extract (PE), the residue separated during the filtration step (PRP byproduct – BP) is no more a waste, but it may now be a promising pharmacological active and/or structuring agent [7–10]. In this aspect, PRP shows one more advantage to be explored, because this compound may undergo a second extraction process, collaborating with three Rs concept (reduce, reuse and recycle) [11,12]. The PRP and, consequently, its BP and their extracts can be used to influence on the tissue regeneration and granulation. In addition, considering PRP characteristics of natural antibiotic and low cost, makes this drug accessible to the population [13–16] and the healing activity of PRP extract has been shown [17].

The skin is exposed to the environment and it may be easily harmed, resulting in wounds that modify its physiology, especially if the dermis is affected, losing its protective functions [18–20]. This organ corresponds to approximately 16% of the body weight, being the biggest organ of the human body and responsible to cover the entire body surface [19,21]. The wound healing process is simultaneously complex and

organized, governed by a harmonic cascade of biological events that are divided into three phases: inflammatory, proliferative and remodeling [21,22].

Accelerate and aid the healing process of chronic wounds results on the decreasing of the aggravation as the affected local amputation [23,24] and consequently reduces significantly the mortality and financial charges, with this disease [1]. With the research improvement, natural compounds have been studied and tested on the wound healing process stimulation, aiming to develop efficacious drugs, presenting no toxicity and low costs [25,26].

However, though PRP and BP present no toxicity [4], the administration of their hydroalcoholic extracts over the harmed skin or mucosa, may cause contact allergies, ulceration, and difficult the healing process [27]. In this sense, the use of appropriated systems to carrier system these extracts is necessary.

The solid lipid nanoparticles (SLN) are considered one of the most interesting studied colloidal systems on the last years [28]. Their topical application is very interesting as they possesses adhesive properties in contact with the skin, forming an occlusive film during the use, besides reducing the transepidermal water loss, strengthening the damaged tissue restauration [29]. A very important advantage of this kind of systems is the use of physiological lipids to prepare the matrix, which reduce the acute chronic toxicity, as well as being biodegradable [30]. The SLN is composed of only a solid lipid or by the mixture of solid lipids in water, which stabilizes using surfactant [31]. Differently, the nanostructured lipid carriers (NLC), a category of lipid nanoparticles (LN), are prepared mixing solid and liquid lipids [32]. In this context, the PRP incorporation on the LN should be of great interest, as it allows a higher structuration of the lipid system, due to its high wax and resin content [33], and also the

particulate system, could permit to protect and modify the release of the extract components over the skin [4,34].

The aim of this study was the preparation and characterization of SLN and NLC containing PRP or BP extracts intended for cutaneous administration for wound healing. Firstly, the extractive solutions were prepared and their physicochemical characteristics evaluated. A formulation study was conducted and, after the preparation of SLN and NLC systems containing the extracts, the morphology, size analyses, cryo-transmission electron microscopy, X-ray diffraction, and propolis loading efficiency have been investigated. Furthermore, the *in vitro* drug release profile of each system was investigated. Finally, the lipid systems were studied in order to understand the influence of the different extracts on occlusive effect, cellular viability, and wound healing.

2. Materials and Methods

2.1 Materials

Propolis (PRP) was purchased from an apiary of *Apis mellifera* L. bees located inside a eucalyptus reserve, surrounded by native forest with a predominance of *Baccharis dracunculifolia* (Asteraceae). This type of PRP is classified as 'type BRP', a typical PRP from the northwest of Paraná state, Brazil [35]. Miglyol 812 (Tricaprin, Cremer, Hamburg, Germany) was kindly donated by *Pic Química e Farmacêutica Ltda* (São Paulo, Brazil). Methanol HPLC grade, chrysin (97% purity, analytical standard), poloxamer 188, poloxamer 407, and tristearin (stearic triglyceride) were purchased from Sigma-Aldrich® (St. Louis, USA). All other chemicals were purchased from Synth® (São Paulo, Brazil) and were of analytical grade.

2.2 Preparation and characterization of the extractive solutions

Propolis extractive solution (PE) was obtained by the turbo extraction method [36] with PRP:ethanol (96%, v/v) ratio of 30:70 (w:w), and at 3500 rpm for three cycles of 5 min. The final dispersion was filtered at vacuum through grade 3 filter paper, while the remaining product on the filter surface was the byproduct of propolis (BP). The extract of BP (BPE) was obtained by the same technique, but the BP: ethanol ratio was 50:50 (w/w) [12]. Both PE and BPE were characterized by the same methodologies: pH, density, and alcohol content [37]; dryness residue and total phenol content.

For determination of dryness residue (DR), exactly 10 g of each extractive solution (PE or BPE) were weighed and concentrated on a water bath (100 ºC), with occasional shaking, and dried on the infrared analytical balance (Gehaka, São Paulo, Brazil) at 110 °C and the final weight was designated the DR value. At least three replicates were carried out to estimate the inherent variability of each determination.

The total phenol content (TPC) of each extract was determined by the Folin-Ciocalteau method [38]. The extract aliquot (2 µL) was mixed with 1,0 mL of the Folin-Ciocalteau, 10 mL of purified water, and 6mL of Na_2CO_3 solution (14.06%, w/v). After 15 min, the absorbance was measured by Shimadzu UV-1650PC spectrophotometer (Tokyo, Japan) at wavelength of 760 nm. A valid calibration curve with solutions of gallic acid was used as reference [39]. TPC was expressed as percentage of total phenolic substances in extractive solution and corresponds to mean of six replicates.

PE and BPE were also analyzed by High Performance Liquid Chromatography (HPLC) coupled to a spectrophotometer detector UV-VIS (Agilent Technologies, Santa Clara, CA, USA). An analytical aliquot of 1.0 mL of extractive solution was extracted with 25 mL of ethyl acetate. The acetate fraction was dried using a water bath (40 ºC) and the residue was dissolved in 10.0 mL of methanol. Modified PTFE membrane filter

(pore size of 0.45 μm, Millipore, Bedford, MA, USA) was utilized to filter the solution. An aliquot of the filtrate was injected in a fixed loop injector (Rheodyne VS 7125, 50 μL), which was utilized to carry the sample into the reversed phase Platinium C18 column (150 mm × 4.6 mm i.d., particle size 5 μm, Hypersil BDS, Alltech, USA), at temperature of 20 ± 0.1 °C (Agilent, Santa Clara, USA). The HPLC system consisted of two pumps, an automatic controller of flow, a diode array detector module, column oven, and an integrator system (Agilent, Santa Clara, USA). The mobile phase was isocratic utilizing 70% of methanol and 30% of acetic acid:water (2:98, v/v), previously filtrated through a 0.45μm Millipore membrane filter (East Hills, NY, USA) and degassed by ultrasound. The flow-rate was 1.0 mL/min and the absorbance of the eluate at 310 nm was monitored by 6 min. The PRP concentration in the solution was determined quantifying the marker chrysin using a calibration curve previously validated. The proceedings followed the normative described by the International Conference on Harmonization of Technical Requirements for Registration of Pharmaceuticals for Human Use Q2(R1) [40]. Thus, the tested parameters were: linearity, selectivity, precision, accuracy, detection limit (DL), quantitation limit (QL) and robustness.

2.3 Preparation of nanostructured lipid systems

Solid lipid nanoparticles (SLN) and nanostructured lipid carriers (NLC) were prepared by stirring followed by ultrasonication. For SLN, a volume of 19 mL of poloxamer 188 aqueous dispersion 2.5%, w/w (P188 d) was heated to 75 ºC, poured over the oil phase (1.0 g of melted tristearin). This preparation was submitted to high shear dispersion (Ultra Turrax T25, IKA-Werke GmbH & Co. KG, Staufen, Germany), at 15,000 rpm for 1 min, and then submitted to the sonication step using a sonicator

(Microson™, Ultrasonic cell Disruptor) at 7 KHz for 15 min [41]. After, the dispersion was cooled to room temperature. The NLC were also prepared by this method, but using a oily phase composed of a mixture tristearin:tricaprin (2:1). PE or BPE was incorporated to the lipid phase, during the fusion process, corresponding to 0.1 or 1.4% (w/w) of DR for PE, and 0.1 and 0.8% (w/w) of DR for BPE, according Table 1.

[Table 1]

2.4 Particle size measurements

The hydrodynamic diameter of lipid structures was measured as the average of the particle size and by the polydispersity index (PdI), by Photon Correlation Spectroscopy (PCS) and using a Zetasizer Nano Series, Nano SP90 (Malvern Instruments, Malvern, England). All the measures were performed at 25 ºC with automatic adjust to the incident light beam (90º). Briefly, 100 µL of each formulation were dispersed in 900 µL of bidistilled water. The samples were homogenized in vortex at 15 Hz, poured into cuvettes and analyzed in triplicate at time 0, 1, 8, 15, 30, 60, and 90 days after preparation [42]. Data were analyzed using the "CONTIN" method [43].

2.5 Cryo-transmission electron microscopy (Cryo-TEM)

The samples of SLN and LNC were vitrified according to previous studies [44]. Briefly, a drop of each sample was placed on a pure copper grid, forming a subtle sample film over the grid's pores. The samples were frozen by rapid immersion in liquid ethane and cooled to around -183 ºC in liquid nitrogen, under temperature control. This was maintained and monitored on the preparation chamber during the

sample preparation. After the lipid dispersion freezing, the remaining ethane was removed with absorbing paper.

The vitrified specimen was transferred to a Zeiss EM922Omega (Carl Zeiss Microscopy, Oberkochen, Germany) transmission electron microscope using a cryoholder (CT3500, Gatan, Munich, Germany). Sample temperature was kept below 100K throughout the examination. Specimens were examined with reduced doses of about 1000-2000 e/nm^2 at 200 kV. Images were recorded by a CCD digital camera (Ultrascan 1000, Gatan, Munich, Germany) and analyzed using a GMS 1.8 software (Gatan, Munich, Germany) [41].

2.6 X-ray diffraction measurements

The nanostructured lipid systems, their constituents, and the extracts (PE and BPE) were analyzed using an X-ray diffractometer (Bruker D-8 Advance, Billerica, USA), under monochromatic radiation $CuK\alpha$ (λ = 1,5406 Å). The diffraction data were collected at room temperature, in an angular sweep 2θ from 1 to 60º with intervals of 0.02º at each 2 s [45]. PE and BPE were dried until constant weight before the analysis.

2.7 Determination of propolis-loading efficiency

To evaluate the content and the entrapment efficiency (EE), a volume of 500 µL of LN was centrifuged (8000 rpm, 20 min), using microtube with coupled micro filter (Amicon® Ultra – 0.5 mL centrifugal filter unit with Ultracel® - 10K membrane, NMWL 10 kDa, Millipore, Darmstadt, Germany). After centrifugation, 100 µL of the lipid phase retained in the filter were diluted in methanol (1:10). This dispersion was submitted to magnetic stirring, in ice bath, for 3 h to the particle breaking and consequent extraction of the active [46]. Then, 1 mL of this extraction was filtered in

micro filter and analyzed by HPLC using the method previously described. The EE (%, w/w) was determined by the quotient of polyphenol content in formulation by the theoretical polyphenols content (%, w/w) times 100.

2.8 In vitro propolis release from systems

The propolis release studies were carried out using Franz's cells [47,48], associated with nylon membranes (Millipore, 0.2 μm pore size). The nylon membranes were rehydrated in purified water at room temperature, at least, 24 h before the cell preparation. The glass Franz's cells had 1 cm diameter, representing an exposition area of 0.78 cm^2 in contact with the receiving phase (5.0 mL), which was composed of ultrapurified water:ethanol (80:20, w/w), in sink condition. This system was maintained under constant magnetic stirring (450 rpm) and the temperature was 32 ± 1 ºC, controlled by a thermostatically controlled bath [42]. The amount of 500 μL of each formulation (nanostructured lipid systems, PE or BPE) was placed in the donor chamber. To perform the free PE and BPE release, extracts dispersions (4%, v/v) were prepared in purified water, so the release membrane was not obstructed, guaranteeing the sink conditions [4,49,50]. At predetermined time intervals (0,5; 1; 2; 4; 6; 8; and 24 h), 300 μL were collected, with immediate reposition of the release medium. The samples were filtered and analyzed by HPLC using the method previously described.

PRP-release kinetic from the formulations was analyzed by plotting the measured chrysin content in the release solution with the time. The data generated from the release studies were fitted to the general release equation, using logarithmic transformations and least-squares regression analysis [51,52], in order to investigate the mechanism of PRP release, as follows:

$$\frac{Mt}{M\infty} = k.t^n \quad (1)$$

where M is the amount of drug released at time t, M_∞ is the total drug content, k is a constant incorporating structural and geometric characteristic of the device, and n is the release exponent, which may indicate the mechanism of drug release.

2.9 In vitro analysis of the occlusive effect

The investigation of the occlusive potential of formulations was performed by a variation of the method proposed by De Vringer [53], which is based on the water evaporation through a membrane and the determination of F factor (occlusion factor). Briefly, 40 g of purified water were placed into a glass flask (4.0 cm diameter and 4.7 cm high) and the open end (area of 12.57 cm^2) was covered by filter paper. The amount of 15.9 mg/cm^2 of the sample was uniformly spread over the membrane. The set (formulation + flask + water + membrane) was stored at 30 ± 1 ºC and relative humidity of 50 - 55%. At predetermined time intervals (0, 6, 24 and 48 h), the samples were weighted and for all formulations, at least, three replicates were analyzed. The F factor was calculated as follows [54].

$$F = 100.\frac{A - B}{A} \quad (2)$$

where F is the occlusion factor (%), A is the mass (g) of water that went through the membrane, and B is the mass (g) of water with formulation that went through the membrane.

2.10 Cellular Viability

Human immortalized keratinocytes (HaCaT cells) (Clonetic, BioWittaker, Wokingham, Berkshire, UK) were cultivated in high glucose concentration, Dulbecco modified Eagle's medium (DMEM) supplemented with 10% of fetal bovine serum

(FBS), penicillin (100 U/mL), streptomycin (100 μg/mL) and 2 mM of L-glutamin (Lonza, Milan, Italy). The cells were incubated at 37 ºC for 24 h in atmosphere with 5% of carbon dioxide, until they reached 80% of confluence. The cell suspensions were counted in Burker chamber and subdivided according with the different treatments in Petri dishes, containing 10^6 cells/mL, in each plaque, and maintained in 2% FBS media overnight for synchronization [55,56].

The cells were separately treated, 24 h before the test begin, with the following formulations: ethanol 70% (w/w, 3 – 60 μL), PE (3 – 60 μL, corresponding to 42.6 – 852 μg/mL of polyphenols), BPE (4 – 80 μL, corresponding to 12 – 240 μg/mL of polyphenols), SLN-B (62.5 – 1000 μL) e SLN-2 (62.5 – 1000 μL, equivalent to 15.07–241.17 μg/mL of polyphenols) diluted in DMEM, without FBS. The control was maintained in DMEM with no formulation for the same time. The analyses were performed using the cytofluorimetric assay Muse Count & Viability Kit (Millipore Corporation, Billerica, MA, USA). Briefly, 380 μL of Muse Count & Viability working solution was added to cells and 20 μL of this cell suspension was incubated for 5 min at room temperature in the dark place. The results are expressed in % of live cells, and the same parameters were employed for the control [56].

2.11 Wound closure test

Hairless female SKH-1 mice (6 weeks old) were purchased from Orient Bio Inc. (Gyeonggi-do, Korea) and lodged in individual plastic cages at temperature and humidity-controlled conditions (22 ± 1 °C, RH 50–60%, 12 h light/dark cycle) with free access to distilled water and food. Mice were acclimated for 10 days before initiation of the treatment. Mice (n = 3). The animals were randomly selected at the start of the

experiment and they were used in accordance with animal protocols approved by the Kyung Hee University Institutional Animal Care and Use Committee.

The animal back skin was compressed and folded (anesthesia with isoflurane, sterile biopsy of 3.5 mm diameter, Miltex Instrument Company, York, PA, USA), under the shoulder, to obtain six identical round wounds on each animal [57,58]. This area was chosen so that the animals cannot reach the region, thus they could not lick or irritate the lesions. The amount of 15% (w/w) of poloxamer 407 was added to each formulation to improve the rheological characteristics of administration [59]. The samples were applied to the wounds and they were digitally photographed daily, including the first day of the treatment. To quantify the wound closure, the software Canvas 11SE (Deneba, Miami, FL, USA) was utilized. The wound closure (*WC*%) rate was calculated as follows:

$$WC(\%) = \frac{WA_d}{WA_0}.100 \quad (3)$$

where WC(%) is the wound closure ratio, WA_d is the wound area at the different days of test and WA_0 is the wound area at day zero.

2.12 Statistical Analysis

All the experiments were performed, at least, in triplicate and the data of each determination were analyzed by mean and standard deviation (mean ± SD). For all results, a value of $p < 0.05$ was taken to denote significance and the software Statistica 10 (StatSoft Company, Tulsa, OK, USA) was utilized to perform the Analysis of Variance (ANOVA) and t-test. In all cases of ANOVA analysis, *post hoc* comparisons of the means of individual groups were performed using Tukey's Honestly Significant Difference test.

3. Results and Discussion

The use of wound healing agents is very important in the treatment of many disorders [17,23,24] and PRP has been much used for this goal [3,6]. However, the main PRP dosage form is the ethanolic extract [60], which displays many disadvantages such as high ethanol concentration and unfavorable rheological and drug release characteristics [4,39,49,50]. These disadvantages result in difficulties on the patient compliance and the therapeutics is also committed. Moreover, BP is the waste material from preparation of PRP extracts, which is normally discarded, but can be utilized as a natural material for the development of nanostructured systems [10,12,61]. Therefore, nanostructured lipid systems could be used to release PRP. In this work, we have evaluated the use of SLN and NLC for release of PE and PBE, with the aim to evaluate the lipid system and extract for wound healing.

3.1 Characterization of propolis and propolis byproduct extracts

The extractive solutions (PE and BPE) were obtained by the turbo-extraction method, which is efficient to obtain extracts of PRP [4,39,50,60,62] To guarantee the applicability of this methodology and the characteristics of standardized PE and BPE, the physicochemical properties regards to the quality of this extracts was performed [39,60]. The results displayed the quality characteristics of extractive solutions (Table 2) [10,12,34,50,61,63,64].

[Table 2]

PE and BPE showed statistically different results for all characteristics. The pH of BPE was higher than of PE, being directly related to the amount of solvent and PRP in the extract [61,64]. Therefore, the difference between the pH values of the two extracts, beyond the amount of ethanol, is based on the phenolic substances, cinnamic alcohol derivatives, nitrogenous substances like aminoacids, among others which balance the pH conducing to a value near six [64]. For PE and BPE, the pH values were compatible with the pH of human body fluids and, therefore, with the clinical utilization of them.

The BPE's relative density and the DR displayed values lower than the ones found for PE, and these can be explained by the loss of soluble substances in ethanol during the first extraction (preparation of PE) [10,12,61]. Moreover, TPC of BPE was more than four times lower than the value found for PE. However, this result shows the polyphenolic substances are still present in BPE, suggesting that many active substances present in PRP still persist in BP [10].

The alcohol content in BPE was also lower than in PE, considering this extract was produced with less ethanol (50%, w/w) than PE (70%, w/w). Moreover, when PE was prepared, the substances with higher affinity to the solvent were carried. The lipid substances, such as waxes, are less attracted to the ethanol, thus concentrating in the BP [10,12,61].

The extractive solutions were also analyzed by HPLC. The chromatographic methodology was validated in order to guarantee that the analytical method provided reliable and reproducible data of the samples [65]. In this context, chrysin was the representative standard (marker) for the polyphenolics substances present in PE and BPE [66]. The method was selective (Figure 1) and showed linearity on all the tested concentrations (n = 10) (0.098; 0.19; 0.39; 0.78; 1.56; 3.13; 6.25; 12.5; 25 and 50

μg/mL), with a representative linear equation of y = 163.2x – 9.5861, and correlation coefficient (r) of 0.9999. For the residues analysis, the calculated F was higher than the critical F (342838.72 > $3{,}675 \times 10^{-94}$; $p < 0.05$) and the regression was highly significant. The detection limit was 0.00536 μg/mL, while the quantification limit, in other words, the least chrysin quantity that is possible to be precisely quantified by this method, was 0.01698 μg/mL [40].

(Figure 1)

Table 3 shows the statistical data for validation of the method. The precision was expressed by the relative standard deviation (RSD, %) of a series of measurements (n = 3) [40]. The resulting data showed relative standard deviation less than 5%, either for repeatability or the intermediate precision. The one-way ANOVA showed no difference between the analysis intra-day, inter-day or even with different analysts ($p > 0.05$), confirming the precision of the method. The accuracy was determined by the analysis of the difference between the average value found and the theoretical one from the chrysin solutions, which were known concentrations (n= 3). The method was capable of a chrysin recovery of 98.95 ± 1.05%. This result is into the limit established by the ICH that is from 80 to 120% of the theoretical concentration. Evaluating the robustness, the varied parameters were the wavelength from 310 to 290 nm, and the flow from 1.0 to 0.8 mL/min. The ANOVA displayed significant difference in the concentrations (μg/mL), when the 290 nm was used on the concentration of 50.0 μg/mL. However, the other concentrations, and when the mobile phase rate was changed, the method was robust.

[Table 3]

3.2 Preparation and particle size analysis of systems

The amounts of extractive solutions added to the SLN and NLC were measured in volume, but corresponding to the DR (w/w) of the extracts. Therefore, the volume of 200 µL, corresponding to DR 0.1% (w/w) of PE or BPE, was incorporated directly to the lipid phase. However, when amounts of extracts were increased to DR 1.4 % (w/w) of PE or 0.8% (w/w) of BPE, it was not possible to add them directly to the lipid phase, due to higher volume. Therefore, it was necessary to concentrate the extract by evaporating of the solvent in order to continue de preparation of the systems, as the ethanol can interfere with the particle stability [67]. In this sense, a previous volume reduction of the extract, from 425 to 200 µL, was performed at controlled temperature (40 ºC). The final amount was then added drop wise over the lipid phase, during its melting.

The size analysis of the systems was performed for 90 days (Figure 2) and allowed to investigate the behavior of the average particle diameter during this time frame, which may influence on the drug release rate, and might be related to the entrapment efficiency [68,69]. All the formulations were classified as nanoparticles, as the highest measured dimension was 336.27 ± 0.94 nm (SLN-4) at 60 days [70]. The mean diameter presented by these particles (higher than 100 nm) is interesting for a potential topical application, as particles that are too small may infiltrate in the deeper layers under the skin, and can lead to systemic effects [71,72].

[Figure 2]

PdI describes the deviation in function to the correlation of the diameter of the formulation on 0, 8, 15, 30, 60 and 90 days (Figure 2). The SLN-1, maintained an index

lower than 0.3 during all the analyzed times, being so monodisperse [73,74]. The SLN-B and SLN-3 kept a PdI of 0.33 and 0.35, respectively. Moreover, SLN-4 displayed an increase of the PdI from 30 days on, resulting in a bidisperse system. This polydispersion may be due to the presence of resins, gums and/or waxes from BPE, which were seen macroscopically, that were not entrapped, lying in between the nanoparticles. Differently, SLN-2 presented a pronounced increase of PdI between 8th and 15th days, and at the final PdI was 0.35. This variation of the index can be also associated to the presence of insoluble substances in the PE. However, the deposition of those substances was not macroscopically visible. In addition, although the SLN with lower active concentrations (SLN-1 and SLN-3) showed stable and monodisperse granulometric profiles, after 90 days they presented big elastic lumps.

Differently from the SLN, the NLC presented unstable profiles. The NLC-1 and NLC-2 showed a growth of 62.88% and 46.43%, respectively, in relation to NLC-B diameter and on day 0. The carriers prepared with BPE (NLC-3 and NLC-4) displayed a decrease on their dimensions of 57.00% and 68.50%, respectively. The blank formulation (NLC-B) showed an increase of size from the beginning of the analysis, but from the day 15th the size did not change, evidencing that the presence of the active compounds influenced on the NLC size behavior.

Due to the presence of lumps on the SLN with the lower concentrations, SLN-2 and SLN-4 were chosen to the following experiments. For a better comparison of the results between SLN and NLC, the carriers NLC-2 and NLC-4 were also chosen.

3.3 Cryo-TEM analysis

The formulations were analyzed by cryo-TEM (Figure 3) aiming to examine the particle dimension individually and the morphology of the structures. Figure 3A and 3B

show, respectively, the NLC-B and SLN-B. Both systems displayed homogenous distribution, but their diameter are between 150 and 200 nm, corroborating with the results found by PCS. Moreover, the particles displayed elongated circular or deformed hexagonal shape, and when observed laterally, they resemble black needles. These were more elliptic on the NLC-B, probably by the presence of tricaprin, a liquid lipid at room temperature, which allows the formation of caps on the surface of the lipid carriers [42,46,75].

[Figure 3]

Relevant differences of morphology were not observed between the blank systems and the ones containing the PRP extracts. Therefore, it may be suggested that the PRP active compounds did not interfered on the morphology of the particles. However, in Figure 3E and 3F, it was possible to observe the presence of an internal lamellar structure from the tristearin, highlighted on the images. NLC-4 (Figure 3E) displayed a structure called “sandwich”, due to the presence of caps around the tristearin lamellar layout, justified by the presence of tricaprin, forming the structure of the NLC and corroborating with other works of this same research area [42].

3.4 X-ray diffraction measurements

The X-ray diffraction technique is extremely important to determine the polymorphic structure present in SLN, or even to differentiate the amorphous material from the crystalline ones, evaluating the influence of liquid lipids on the NLC [76]. In this context, the physical mixtures, as well as the components separately of the selected formulations were analyzed (Figure 4). Poloxamer 188 showed two characteristic peaks

in approximately 19 and 23º, confirming the profile demonstrated in other studies [77,78]. This surfactant is characterized as a non-ionic polymer, which may be employed as emulsifying agent, dispersing agent and wetting agent on the chemical or pharmaceutical industries [37,77,79]. The peaks of tristearin were observed in 2º; 5.9º; 21.5º and 23.4º and are according to the literature [78,80]. Moreover, both the extractive solutions (PE and BPE) displayed a peak around 22º (dashed line). This is designated as a typical PRP (*in natura*) peak, corresponding to the diffraction of the reflection of the glassy amorphous surface [81]. The presence of this peak for the extracts indicates the constancy on the presence of PRP components in the extracts. Besides, the diffractometric profile evidenced on the PRP (*in natura*) studied by Drapak et al. [81] is similar with the ones obtained for PE and BPE in this study.

[Figure 4]

After the studies of the individualized compounds, the formulations were studied and also their physical mixture (PM) (Figure 5). When comparing the PM of the blank particles (PM-B) with the SLN-B or NLC-B, it is observed that the blank nanoparticles evidenced a reduction on the signals, taking almost to disappearance of the peak in 21.5º corresponding to the tristearin, which may indicate an interaction of the lipid with the formulation. The peaks on the beginning of the spectra (2º and 6º), indicates, according to other studies, that the triglycerides are arranged in lamellar phase [46,76]. In addition, PM containing PE (PM-PE) or BPE (PM-BPE) displayed a peak in approximately 21.5º, being related to tristearin or the extracts. This peak appeared on the diffractograms of SLN-2, SLN-4, NLC-2 and NLC-4, suggesting that the active agents may have been completely incorporated within the system.

[Figure 5]

With the application of this technique, it was confirmed the presence of lower peaks (2º and 6º) on the SLN and NLC, proposing that the lipids organize in lamellar phase. In addition, it may be suggested that the extracts did not alter the lipid nanoparticles, in comparison to the blank ones, indicating that the order of the hydrocarbons chain is kept intact [46]. NLC diffractograms presented more amorphous phase, probably due to the presence of tricaprin [76].

3.5 Determination of propolis-loading efficiency

HPLC was utilized to analyze the PRP loading (EE) in the lipid systems, in terms of chrysin content (Table 3). The knowledge and evaluation of the PRP content, as well as the EE, in each formulation is fundamental for the development of a drug delivery system [34,49]. Both SLN and NLC containing BPE displayed highest EE. It is suggested that a higher affinity of the lipids of these formulations by BPE, considering the wax content present in the BP is higher than the PRP one [10,12,61]. Thus, these lipid constituents of BPE might be interacting synergistically with the formulation, favoring the entrapment of most active substances (e.g. chrysin marker). In this way, the lipid substances present in a greater amount in BPE facilitating the extract encapsulation [82].

Comparing the systems containing PE (SLN-2 and NLC-2), it was observed that the EE of SLN was higher than of NLC. On the other hand, for the systems containing BPE, NLC-4 showed the highest EE. In this sense, it may be inferred that the NLC improved the BPE EE, probably due to the higher interaction with the particle lipid phase, constituted by a mixture of lipids solid and liquid, with the BPE fatty phase, as

the carriers allow the formation of a less rigid structure, promoting the entrapment of fat-soluble substances [46].

3.6 In vitro drug release

For the *in vitro* drug release investigation of the lipid systems, it was used Franz's cell [83]. The lipid system was kept under magnetic stirring on thermostatic bath. In predetermined time intervals, equal volumes of the release medium were collected and then chrysin marker was quantified by HPLC, obtaining a release profile according to the time. The receptor medium was prepared with purified water:ethanol (80:20), pH of 7,2 and the temperature was 32 ± 0.5 ºC, to resemble the external body temperature [84–86]. The use of a hydro-alcoholic solution is justified by the fact that the formulation is made of lipid [87].

The Figure 6 shows the release profile of the PE free and incorporated in lipid systems. Chrysin release profile from the extracts was faster than from all lipid systems, highlighting that either SLN or NLC modified the drug release profile, reducing its release rate. Moreover, the SLN-2 showed the slowest release rate. SLN-4 and NLC-4 showed the fasted chrysin release (11.06 ± 0.31% and 13.36 ± 0.62% in 24 h, respectively), while the systems containing PE released 1.55 ± 0.10% (SLN-2) and 2.84 ± 0.15% (NLC-2) of chrysin during 24 h.

[Figure 6]

The SLN displayed a lower chrysin release compared to the NLC, suggesting that this more rigid structure sustained the active inside the particle for longer time, or that the main amount of the extract substances was in the core of the SLN [88,89].

The results from the investigation of the chrysin release kinetics from the extracts and from the nanostructured lipid systems are displayed in Table 4. For both SLN and NLC was considered the spherical morphology and results for the *n* were lower than 0.5, indicating that the drug release was governed by Fickian diffusion. This result was expected as lipid matrixes are classified, most of the times as inert, because in contact with water they do not modify their structure [90]. The PE and BPE showed a value of *n* slightly higher than 0.5, indicating a kinetic governed by diffusion phenomenon and polymeric chain relaxation [91], which may be attributed to the resins and gums present in the extract [50,92].

[Table 4]

3.7 In vitro occlusive effect of the lipid systems

The *in vitro* occlusion test is based on the water evaporation through a paper membrane and is measured by the occlusion factor (*F*). Formulations constituted by smaller particles, usually present higher occlusion factor [53]. Thus, the influence of the dimension may be observed when comparing the occlusive power of SLN-B and NLC-B. This presented a dimensional average lower than the SLN-B, throughout the 90 days of analysis, showed a higher *F*, on the times of 24 and 48 h (Figure 7). However, the presence of the different extracts, added to their interaction with the lipid systems, led to results that were not only dependent of the granulometry of the formulations.

[Figure 7]

The particles containing PE (SLN-2 and NLC-2), presented the highest *F* in 24 and 48 h, indicating the presence of resins, gums and waxes (coming from the PE); thus, providing a lower water permeability to the system. Moreover, there were no statistical differences between the carrier and the SLN in all times ($p > 0.05$), evidencing that PE was the main factor that influenced significantly the occlusion characteristic.

Therefore, despite the low lipid concentration used in the composition of the nanoparticulate system, the PE associated to the oily fraction of the formulations was capable of grant a greater occlusive function to the LN. This result shows itself interesting when thinking of a topic administration for wound healing, once the high occlusive capacity enhances the affected site hydration and consequently, aids on the tissue recovering [93,94].

The increase on hydration at the site on contact with a lipid nanoparticulate formulation occurs by the formation of an adhesive film, which hinder the water evaporation [53,95,96]. In this work, this occlusive effect was enriched by the PE that has great content of resins, which favors adhesive characteristics to the formulations [3]. In this sense, harmonious hydration characteristics are key properties to the developments of innovative formulations to the acceleration of the healing process [93].

3.8 Cellular viability

This methodology is based on the microcapillary cytometry with fluorescence detection, allowing the analysis of individual cells, determining the count of viable cells [56]. Thus, it was possible to verify if the lipid systems maintained the HaCat viable, or if they hindered their viability. In this study, the SLN-2 was selected, as it was very promising to a topical utilization, looking to its occlusive potential, as well as showing a

stable dimensional profile. The SLN-B was also evaluated to check the effect of the blank formulation over the cells (Figure 8).

[Figure 8]

The Figure 8a presents the cell viability for SLN-B, which presented lower viability than the control, showing a high quantity of dead cells, especially at the two highest concentrations. In addition, SLN-2 viability (Figure 8b) was really close to the control, being higher than the SLN-B. Thus, it is suggested that the presence of PE aided on this parameter.

PE and BPE were also evaluated in order to investigate their influence on cell viability. The ethanol (70%, w/w) was tested to analyze the influence of this vehicle on the extracts. These three samples were tested on a maximum concentration of 2% (v/v) of ethanol. So the concentrations were 0.1%, 0.2%, 1% and 2% that corresponded to the volumes of 3, 6, 30 and 60 µL of PE or ethanol, and 4, 8, 40 an 80 µL of BPE. Thus, the PE correspondent concentrations of polyphenols were from 42.6 to 852 µg/mL, while for the BPE they ranged from 12 to 240 µg/mL. PE presented highest cell viability, once that in all the tested concentrations the amount of viable cells was around 100% (Figure 8c). BPE also displayed good values to this parameter, but lower than PE. The ethanol exhibited mortality greater than the control, especially on the biggest volume tested, being possible to infer that constituents of the extracts helped to maintain the cells viable, and proving that the ethanol was evaporated during the preparation of the systems, as previously described.

3.9 Wound closure test

Selected SLN (SLN-2 and SLN-4), as well as SLN-B were investigated. Starting at day 0 (d0) to day 15 (d15), the wound closure was calculated related to the original wound area (Figure 9).

[Figure 9]

The wound closure was higher than 85% on the control and over 89% (Figure 10) for the treatment with SLN-2 and SLN-4 from the 14th (d14) of treatment. When the lesions were treated with SLN containing PE or BPE, an increase on the wound size was observed during the first three days. This may be due to an over expression of inflammation mediators, with infiltrated of polymorphonuclear leukocytes, during the inflammatory phase during the healing process [97]. On the other hand, after this period, from d7 on a better evolution of the healing process [20] occurred with the treatment using the formulations containing PE or BPE to a complete restoration of the lesion. There were no significant differences ($p > 0.05$) between these two treatments. These results are according to investigations, which reported the acceleration of the healing process from this time frame of treatment [17,97–99].

[Figure 10]

4. Conclusions

The present study demonstrated the development of solid lipid nanoparticles and nanostructured lipid carriers to nano-encapsulate propolis. For the first time, nanostructured lipid systems could be successfully obtained using the residue obtained

from the preparation of propolis extract, which is normally discarded. The characteristics (e.g. morphology, size, drug loading and release profile) of the formulations were adversely affected by blend of propolis extractive solution (propolis or byproduct) and lipid system (solid lipid nanoparticles or nanostructured lipid carriers) promoted significant differences in the nanoparticles. In which the SLN showed greater granulometric stability than the NLC.

Likewise, when evaluated the occlusive formulations' properties, it was possible to observe that the PE was a determinant factor to enhance the LN occlusion potential. This, the dispersion SLN-2 generates higher expectation when putting together its granulometric stability and the occlusive power comparing to NLC-2, which also contains PE. Moreover, the biological investigation showed that the lipid formulation containing PE (SLN-2) presented great cell viability and on the *in vivo* test, the same lipid formulation containing the different extracts (PE on SLN-2 and BPE on SLN-4) displayed promising capacity of accelerating the wound healing process.

Therefore, considering the results obtained and the principle of sustainability (reduce, reuse and recycle), this work could represent an important improvement in terms of materials, active agents and formulation for wound healing. However, further research is needed to gain a better understanding about the properties of these formulations for future *in vivo* preclinical and clinical studies.

Conflict of interest

The author(s) confirm that this article content has no conflict of interest.

Acknowledgements

The authors are grateful to CNPq (*Conselho Nacional de Pesquisa*/National Research Council; Process nº 470965/2013-4), CAPES (*Coordenação de Aperfeiçoamento de Pessoal de Nível Superior*/Coordination for the Improvement of Higher Education), and FINEP (*Financiadora de Estudos e Projetos*/Financier of Studies and Projects) for their financial support.

References

[1] F.R. Henshaw, T. Bolton, V. Nube, A. Hood, D. Veldhoen, L. Pfrunder, G.L. McKew, C. MacLeod, S. V. McLennan, S.M. Twigg, Topical application of the bee hive protectant propolis is well tolerated and improves human diabetic foot ulcer healing in a prospective feasibility study, J. Diabetes Complications. 28 (2014) 850–857.

[2] M.C. Marcucci, Propolis: chemical composition, biological properties and therapeutic activity, Apidologie. 26 (1995) 83–99.

[3] G.A. Burdock, Review of the Biological Properties and Toxicity of Bee Propolis (Propolis), Food Chem. Toxicol. 36 (1998) 347–363.

[4] M.L. Bruschi, D.S. Jones, H. Panzeri, M.P.D. Gremião, O. de Freitas, E.H.G. Lara, Semisolid Systems Containing Propolis for the Treatment of Periodontal Disease: In Vitro Release Kinetics, Syringeability, Rheological, Textural, and Mucoadhesive Properties, J. Pharm. Sci. 96 (2007) 2074–2089.

[5] G. Balata, H.M. El Nahas, S. Radwan, Propolis organogel as a novel topical delivery system for treating wounds, Drug Deliv. 21 (2014) 55–61.

[6] E.L. Ghisalberti, Propolis: A Review, Bee World. 60 (1979) 59–84.

[7] A.V. dos Santos, A.S. Teixeira, P.B. Rodrigues, R.T.F. de Freitas, A.M. Guimarães, R.A. Giacometti, Valor nutritivo do resíduo de própolis para frangos

de corte, Ciência E Agrotecnologia. 27 (2003) 1152–1159.

[8] B.R. Pezzini, M.A.S.S. Silva, H.G. Ferraz, Formas farmacêuticas sólidas orais de liberação prolongada: sistemas monolíticos e multiparticulados, Rev. Bras. Ciências Farm. 43 (2007).

[9] E.L. Santos, F. Cristiano, E.C. Pontes, R.C. Lira, M.C.A. Cavalcanti, Resíduo do processamento do extrato de própolis vermelha em ração comercial para alevinos de Tilápia do Nilo (Oreochromis niloticus), 4 (2013) 179–185.

[10] L.A.S. Toledo, M.I. Bavato, H.C. Rosseto, R. Cortesi, M.L. Bruschi, Pharmaceutical films made from the waste material from the preparation of propolis extracts: development and characterization, Brazilian J. Pharm. Sci. 51 (2015) 847–859.

[11] M. Larney, A.M. van Aardt, Case study: Apparel industry waste management: a focus on recycling in South Africa, Waste Manag. Res. 28 (2010) 36–43.

[12] L.A.S. Toledo, H.C. Rosseto, L. Ravani, R. Cortesi, M.L. Bruschi, Waste Material of Propolis as a Film Forming Agent Intended to Modify the Metronidazole Release: Preparation and Characterization, Curr. Drug Deliv. 13 (2016) 1152–1164.

[13] C. de L.E. Bernardo, I.A.F. de Souza, C. Colavitti, C. Garcia, Própolis: cicatrizante e antibiótico natural, Rev. Bras. Enferm. 43 (1990) 101–106.

[14] J.M. Sforcin, A. Fernandes, C.A. Lopes, V. Bankova, S.R. Funari, Seasonal effect on Brazilian propolis antibacterial activity., J. Ethnopharmacol. 73 (2000) 243–249.

[15] M.H. Barbosa, F.B. Zuffi, H.B. Maruxo, L.L.R. Jorge, Ação terapêutica da própolis em lesões cutâneas, Acta Paul. Enferm. 22 (2009) 318–322.

[16] R. Silva-Carvalho, F. Baltazar, C. Almeida-Aguiar, Propolis: A Complex Natural

Product with a Plethora of Biological Activities That Can Be Explored for Drug Development., Evid. Based. Complement. Alternat. Med. 2015 (2015).

[17] E. Sehn, L. Hernandes, S.L. Franco, C.C.M. Gonçalves, M.L. Baesso, Dynamics of reepithelialisation and penetration rate of a bee propolis formulation during cutaneous wounds healing, Anal. Chim. Acta. 635 (2009) 115–120.

[18] G. Jin, J. Li, K. Li, Photosensitive semiconducting polymer-incorporated nanofibers for promoting the regeneration of skin wound, Mater. Sci. Eng. C. 70 (2017) 1176–1181.

[19] C. Isaac, P.R.S. de Ladeira, F.M.P. do Rêgo, J.C.B. Aldunate, M.C. Ferreira, Processo de cura das feridas: cicatrização fisiológica, Rev. Med. 89 (2010) 125–131.

[20] F.E.L. PEREIRA, Degenerações, morte celular, lesões do interstício, cicatrização, regeneração, in: G.B. FILHO (Ed.), Bogliolo Patol., 8th ed., Guanabara Koogan, Belo Horizonte, 2011: pp. 77–132.

[21] L.C. Junqueira, J. Carneiro, Histologia Básica, 12th ed., Guanabara Koogan, Rio de Janeiro, 2013.

[22] P.A. Coulombe, Towards a Molecular Definition of Keratinocyte Activation after Acute Injury to Stratified Epithelia, Biochem. Biophys. Res. Commun. 236 (1997) 231–238.

[23] I. Ammar, S. Bardaa, M. Mzid, Z. Sahnoun, T. Rebaii, International Journal of Biological Macromolecules Antioxidant , antibacterial and in vivo dermal wound healing effects of Opuntia flower extracts, Int. J. Biol. Macromol. 81 (2015) 483–490.

[24] Y.J.J. Rhou, F.R. Henshaw, M.J. McGill, S.M. Twigg, Congestive heart failure presence predicts delayed healing of foot ulcers in diabetes: An audit from a

multidisciplinary high-risk foot clinic, J. Diabetes Complications. 29 (2015) 556–562.

[25] D.E. Tsala, D. Amadou, S. Habtemariam, Natural wound healing and bioactive natural products, Phytopharmacology. 4 (2013) 532–560.

[26] R.F. Pereira, P.J. Bártolo, Traditional Therapies for Skin Wound Healing., Adv. Wound Care. 5 (2016) 208–229.

[27] K.D. Hay, D.E. Greig, Propolis allergy: a cause of oral mucositis with ulceration., Oral Surg. Oral Med. Oral Pathol. 70 (1990) 584–586.

[28] M. Paranjpe, J.H. Finke, C. Richter, T. Gothsch, A. Kwade, S. Büttgenbach, C.C. Müller-Goymann, Physicochemical characterization of sildenafil-loaded solid lipid nanoparticle dispersions (SLN) for pulmonary application, Int. J. Pharm. 476 (2014) 41–49.

[29] B.W. Müller, Topische Mikroemulsionen als neue Wirkstoff-Traègersysteme, in: R.H. Müller, G.E. Hildebrand (Eds.), Pharm. Technol. Mod. Arzneiformen, 2nd ed., Wissenschaftliche Verlagsgesellschaft, Stuttgart, 1998: pp. 161 – 168.

[30] C. Freitas, R.H. Müller, Effect of light and temperature on zeta potential and physical stability in solid lipid nanoparticle (SLN^{TM}) dispersions, Int. J. Pharm. 168 (1998) 221–229.

[31] A. Yaghmur, O. Glatter, Characterization and potential applications of nanostructured aqueous dispersions, Adv. Colloid Interface Sci. 147 (2009) 333–342.

[32] O. Krasodomska, P. Paolicelli, S. Cesa, M.A. Casadei, C. Jungnickel, Protection and viability of fruit seeds oils by nanostructured lipid carrier (NLC) nanosuspensions, J. Colloid Interface Sci. 479 (2016) 25–33.

[33] G. Rassu, M. Cossu, R. Langasco, A. Carta, R. Cavalli, P. Giunchedi, E. Gavini,

Propolis as lipid bioactive nano-carrier for topical nasal drug delivery, Colloids Surfaces B Biointerfaces. 136 (2015) 908–917.

[34] S.B. de S. Ferreira, B.R. de A. Dias, C.S. Obregón, C.C. Gomes, R.R.A. Pereira, J.S.R. Godoy, T.I.E. Svidizinski, M.L. Bruschi, Microparticles containing propolis and metronidazole: in vitro characterization, release study and antimicrobial activity against periodontal pathogens ´, Pharm. Dev. Technol. 19 (2013) 173–180.

[35] M.C. Marcucci, Própolis Tipificada: Um Novo Caminho para a Elaboração de Medicamentos de Origem Natural, Contendo este Produto Apícola, Rev. Fitos. 1 (2006) 36–46.

[36] P.C. List, P.H., Schmidt, Phytopharmaceutical Technology, Heyden & Son, London, 1989.

[37] U. (United S. Pharmacopeia), Validation of Compendial Methods, 33rd ed., United States Pharmacopeial Convention, Rockville, 2008.

[38] E.W. Teixeira, D. Message, G. Negri, A. Salatino, P.C. Stringheta, Seasonal variation, chemical composition and antioxidant activity of Brazilian propolis samples., Evid. Based. Complement. Alternat. Med. 7 (2010) 307–315.

[39] R.R.A. Pereira, J.S.R. Godoy, T.I.E. Svidzinski, M.L. Bruschi, Preparation and Characterization of Mucoadhesive Thermoresponsive Systems Containing Propolis for the Treatment of Vulvovaginal Candidiasis, J. Pharm. Sci. 102 (2013) 1222–1234.

[40] ICH (International Conference on Harmonization of Technical Requirements for Registration of Pharmaceuticals for Human Use, Validation of analytical procedures: text and methodology Q2(R1), (2005).

[41] R. Cortesi, M. Campioni, L. Ravani, M. Drechsler, M. Pinotti, E. Esposito,

Cationic lipid nanosystems as carriers for nucleic acids, N. Biotechnol. 31 (2014) 44–54.

[42] L. Ravani, M.G. Sarpietro, E. Esposito, A. Di Stefano, P. Sozio, M. Calcagno, M. Drechsler, C. Contado, F. Longo, M.C. Giuffrida, F. Castelli, M. Morari, R. Cortesi, Lipid nanocarriers containing a levodopa prodrug with potential antiparkinsonian activity, Mater. Sci. Eng. C. 48 (2015) 294–300.

[43] R. Pecora, Dynamic Light Scattering Measurement of Nanometer Particles in Liquids, J. Nanoparticle Res. 2 (2000) 123–131.

[44] E. Esposito, N. Eblovi, S. Rasi, M. Drechsler, G.M. Di Gregorio, E. Menegatti, R. Cortesi, Lipid-based supramolecular systems for topical application: a preformulatory study., AAPS PharmSci. 5 (2003) 62–76.

[45] Y. Li, N. Taulier, A.M. Rauth, X.Y. Wu, Screening of Lipid Carriers and Characterization of Drug-Polymer-Lipid Interactions for the Rational Design of Polymer-Lipid Hybrid Nanoparticles (PLN), Pharm. Res. 23 (2006) 1877–1887.

[46] E. Esposito, M. Fantin, M. Marti, M. Drechsler, L. Paccamiccio, P. Mariani, E. Sivieri, F. Lain, E. Menegatti, M. Morari, R. Cortesi, Solid Lipid Nanoparticles as Delivery Systems for Bromocriptine, 25 (2008).

[47] C. Nastruzzi, E. Esposito, C. Pastesini, R. Gambari, E. Menegatti, Comparative study on the release kinetics of methyl-nicotinate from topic formulations, Int. J. Pharm. 90 (1993) 43–50.

[48] R. Cortesi, L. Ravani, E. Menegatti, M. Drechsler, E. Esposito, Colloidal dispersions for the delivery of acyclovir: a comparative study., Indian J. Pharm. Sci. 73 (2011) 687–693.

[49] M.L. Bruschi, R.S. Lopes, S.L. Franco, M.P.D. Gremião, In vitro release of propolis from gelatin microparticles prepared by spray-drying technique, Rev.

Bras. Ciências Farm. 25 (2004) 79–84.

[50] M.L. Bruschi, H. Panzeri, O. De Freitas, E. Helena, G. Lara, M. Palmira, D. Gremião, Sistemas de liberação de fármaco intrabolsa periodontal, Rev. Bras. Ciências Farm. 42 (2006) 29–47.

[51] R.W. Korsmeyer, R. Gurny, E. Doelker, P. Buri, N.A. Peppas, Mechanisms of solute release from porous hydrophilic polymers, Int. J. Pharm. 15 (1983) 25–35.

[52] M.L. Bruschi, Strategies to modify the drug release from pharmaceutical systems, 1st ed., Elsevier , Amsterdam, 2015.

[53] T. de Vringer, Topical preparation containing a suspension of solid lipid particles, EP 0506197 A1, 1992.

[54] S.A. Wissing, R.H. Müller, Cosmetic applications for solid lipid nanoparticles (SLN)., Int. J. Pharm. 254 (2003) 65–68.

[55] G. Valacchi, C. Sticozzi, G. Belmonte, F. Cervellati, J. Demaude, N. Chen, Y. Krol, C. Oresajo, Vitamin C Compound Mixtures Prevent Ozone-Induced Oxidative Damage in Human Keratinocytes as Initial Assessment of Pollution Protection, PLoS One. 10 (2015) 1–15.

[56] E. Esposito, C. Sticozzi, L. Ravani, M. Drechsler, X.M. Muresan, F. Cervellati, R. Cortesi, G. Valacchi, Effect of new curcumin-containing nanostructured lipid dispersions on human keratinocytes proliferative responses, Exp. Dermatol. 24 (2015) 449–454.

[57] Y. Lim, A.D. Phung, A.M. Corbacho, H.H. Aung, E. Maioli, A.Z. Reznick, C.E. Cross, P.A. Davis, G. Valacchi, Modulation of cutaneous wound healing by ozone: Differences between young and aged mice, Toxicol. Lett. 160 (2006) 127–134.

[58] G. Valacchi, I. Zanardi, Y. Lim, G. Belmonte, C. Miracco, C. Sticozzi, V. Bocci,

V. Travagli, Ozonated oils as functional dermatological matrices: Effects on the wound healing process using SKH1 mice, Int. J. Pharm. 458 (2013) 65–73.

[59] S.B. De Souza Ferreira, J.B. Da Silva, F.B. Borghi-Pangoni, M.V. Junqueira, M.L. Bruschi, Linear correlation between rheological, mechanical and mucoadhesive properties of polycarbophil polymer blends for biomedical applications, J. Mech. Behav. Biomed. Mater. 68 (2017) 265–275.

[60] M.. Bruschi, M.L.. Cardoso, M.. Lucchesi, M.P.. Gremião, Gelatin microparticles containing propolis obtained by spray-drying technique: preparation and characterization, Int. J. Pharm. 264 (2003) 45–55.

[61] L. De Francisco, Y. Costa, P.M. Outuki, R.P. Souza, P.S. Bonfim-Mendonça, C.R. Novello, M. Consolaro, M.L. Bruschi, Nanoparticles of waste material of propolis and gelatin as a novel system for delivery of L-ascorbic acid., Curr. Drug Deliv. 13 (2016).

[62] S.L. Franco, J.H.F. Bueno, OTIMIZAÇÃO DE PROCESSO EXTRATIVO DE PRÓPOLIS, Infarma - Ciências Farm. 11 (1999) 48–51.

[63] S.L. Franco, M.L. Bruschi, L.P.P. Moura, J.H.. Bueno, Avaliação farmacognóstica da própolis da região de Maringá, Rev. Bras. Farmacogn. 9/10 (2000) 1–10.

[64] M.L. Bruschi, T. Klein, R.S. Lopes, S.L. Franco, M.P.D. Gremião, Contribuição ao protocolo de controle de qualidade da própolis e de seus extratos, Rev. Bras. Ciências Farm. 23 (2002) 289–306.

[65] L. Deprez, P. Corbisier, A.-M. Kortekaas, S. Mazoua, R. Beaz Hidalgo, S. Trapmann, H. Emons, Validation of a digital PCR method for quantification of DNA copy number concentrations by using a certified reference material., Biomol. Detect. Quantif. 9 (2016) 29–39.

[66] M.L. Bruschi, S.L. Franco, M.P.D. Gremião, Application of an HPLC Method for Analysis of Propolis Extract, J. Liq. Chromatogr. Relat. Technol. 26 (2003) 2399–2409.

[67] D.M. Ridolfi, Nanopartículas lipídicas sólidas: Encapsulação de tretinoína para aplicação tópica, Universidade Estadual de Campinas, 2011.

[68] S. Freitas, H.P. Merkle, B. Gander, Microencapsulation by solvent extraction/evaporation: reviewing the state of the art of microsphere preparation process technology, J. Control. Release. 102 (2005) 313–332.

[69] S.-M. Ng, J.-Y. Choi, H.-S. Han, J.-S. Huh, J.O. Lim, Novel microencapsulation of potential drugs with low molecular weight and high hydrophilicity: Hydrogen peroxide as a candidate compound, Int. J. Pharm. 384 (2010) 120–127.

[70] R.H. Müller, K. Mäder, S. Gohla, Solid lipid nanoparticles (SLN) for controlled drug delivery – a review of the state of the art, Eur. J. Pharm. Biopharm. 50 (2000) 161–177.

[71] T.W. Prow, J.E. Grice, L.L. Lin, R. Faye, M. Butler, W. Becker, E.M.T. Wurm, C. Yoong, T.A. Robertson, H.P. Soyer, M.S. Roberts, Nanoparticles and microparticles for skin drug delivery, Adv. Drug Deliv. Rev. 63 (2011) 470–491.

[72] G. Gainza, M. Pastor, J.J. Aguirre, S. Villullas, J.L. Pedraz, R.M. Hernandez, M. Igartua, A novel strategy for the treatment of chronic wounds based on the topical administration of rhEGF-loaded lipid nanoparticles: In vitro bioactivity and in vivo effectiveness in healing-impaired db/db mice, J. Control. Release. 185 (2014) 51–61.

[73] R. Asasutjarit, S. Lorenzen, S. Sirivichayakul, K. Ruxrungtham, U. Ruktanonchai, G.C. Ritthidej, Effect of Solid Lipid Nanoparticles Formulation Compositions on Their Size , Zeta Potential and Potential for In Vitro pHIS-HIV-

Hugag Transfection, 24 (2007) 1098–1107.

[74] A.C.C. Silva, E. González-Mira, M.L.L. García, M.A.A. Egea, J. Fonseca, R. Silva, D. Santos, E.B.B. Souto, D. Ferreira, Colloids and Surfaces B : Biointerfaces Preparation , characterization and biocompatibility studies on risperidone-loaded solid lipid nanoparticles (SLN): High pressure homogenization versus ultrasound, Colloids Surfaces B Biointerfaces. 86 (2011) 158–165.

[75] K. Jores, W. Mehnert, M. Drechsler, H. Bunjes, C. Johann, K. Ma, K. Mäder, Investigations on the structure of solid lipid nanoparticles (SLN) and oil-loaded solid lipid nanoparticles by photon correlation spectroscopy , field-flow fractionation and transmission electron microscopy, J. Control. Release. 95 (2004) 217–227.

[76] E. Esposito, P. Mariani, L. Ravani, C. Contado, M. Volta, S. Bido, M. Drechsler, S. Mazzoni, E. Menegatti, M. Morari, R. Cortesi, Nanoparticulate lipid dispersions for bromocriptine delivery : Characterization and in vivo study, Eur. J. Pharm. Biopharm. 80 (2012) 306–314.

[77] M.A. (Faculdade de C.F. Gouveia, Obtenção e caracterização de dispersões sólidas de nimesulida Obtenção e caracterização de dispersões sólidas de nimesulida, Universidade Estadual de São Paulo, 2011.

[78] V.M. Meyagusku, Desenvolvimento e Caracterização de nanopartículas lipídicas sólidas contendo ciprofloxacino, Universidade Estadual Paulista “Júlio de Mesquita Filho,” 2014.

[79] W. Mehnert, K. Mäder, Solid lipid nanoparticles Production , characterization and applications, 47 (2001) 165–196.

[80] W. MacNaughtan, I.A. Farhat, C. Himawan, V.M. Starov, A.G.F. Stapley, A

differential scanning calorimetry study of the crystallization kinetics of tristearin-tripalmitin mixtures, J. Am. Oil Chem. Soc. 83 (2006) 1–9.

[81] S.I. Drapak, S. V. Gavrylyuk, V.M. Kaminskii, Z.D. Kovalyuk, X-ray diffraction study of the molecular propolis films deposited from an alcohol solution onto the cleavage surfaces of layered V2VI3 compounds, Tech. Phys. 53 (2008) 1215–1221.

[82] A. Dingler, S. Gohla, Production of solid lipid nanoparticles (SLN): scaling up feasibilities, J. Microencapsul. 19 (2002).

[83] T.J. Franz, Percutaneous Absorption. On the Relevance of in Vitro Data, J. Invest. Dermatol. 64 (1975) 190–195.

[84] M.H. Akanda, R. Rai, I.J. Slipper, B.Z. Chowdhry, D. Lamprou, G. Getti, D. Douroumis, Delivery of retinoic acid to LNCap human prostate cancer cells using solid lipid nanoparticles, Int. J. Pharm. 493 (2015) 161–171.

[85] M. Lusina Kregar, M. Dürrigl, A. Rožman, Ž. Jelčić, B. Cetina-Čižmek, J. Filipović-Grčić, Development and validation of an in vitro release method for topical particulate delivery systems, Int. J. Pharm. 485 (2015) 202–214.

[86] F.S.G. Praça, Liberação e permeação in vitro de produtos transdérmicos: um estudo metodológico de aparatos e de condições experimentais, Universidade de São Paulo, 2010.

[87] FDA (Food and drug Administration), Guidance for Industry Nonsterile Semisolid Dosage Forms Scale-Up and Postapproval Changes: Chemistry, Manufacturing, and Controls; In Vitro Release Testing and In Vivo Bioequivalence Documentation Guidance for Industry Nonsterile Semisolid Dosage Forms, (1997).

[88] M. Üner, G. Yener, Importance of solid lipid nanoparticles (SLN) in various

administration routes and future perspectives, Int. J. Nanomedicine. 2 (2007) 289–300.

[89] E.. Souto, S.. Wissing, C.. Barbosa, R.. Müller, Evaluation of the physical stability of SLN and NLC before and after incorporation into hydrogel formulations, Eur. J. Pharm. Biopharm. 58 (2004) 83–90.

[90] C.M. Lopes, J.M.S. Lobo, P. Costa, Formas farmacêuticas de liberação modificada: polímeros hidrifílicos, Rev. Bras. Ciências Farm. 41 (2005) 143–154.

[91] P.L. Ritger, N.A. Peppas, A simple equation for description of solute release II. Fickian and anomalous release from swellable devices, J. Control. Release. 5 (1987) 37–42.

[92] M.L. Bruschi, Desenvolvimento e caracterização de sistemas de liberação de própolis intrabolsa periodontal, Universidade de São Paulo, 2006.

[93] K. Ousey, K.F. Cutting, A.A. Rogers, M.G. Rippon, The importance of hydration in wound healing: reinvigorating the clinical perspective, J. Wound Care. 25 (2016) 122–130.

[94] H. Hamishehkar, S. Same, K. Adibkia, K. Zarza, J. Shokri, M. Taghaee, M. Kouhsoltani, A comparative histological study on the skin occlusion performance of a cream made of solid lipid nanoparticles and Vaseline., Res. Pharm. Sci. 10 (2015) 378–387.

[95] S.A. Wissing, A. Lippacher, R.H. Muller, Investigations on the occlusive properties of solid lipid nanoparticles (SLN), 324 (2001) 313–324.

[96] S.A. Wissing, R.H. Muller, Solid lipid nanoparticles as carrier for sunscreens : in vitro release and in vivo skin penetration, 81 (2002) 225–233.

[97] S.C. Rahal, A.P.F.R.. Bracarense, C.Y. Tanaka, T.P. Grillo, C.A.. Leite,

Utilização de própolis ou mel no tratamento de feridas iduzidas em ratos, Arch. Veterninary Sci. 8 (2003) 61–67.

[98] A. Aa, O. Aa, The healing potential of honey and propolis lotion on septic wounds, Asian Pacific J. Trop. Biomed. Asian Pacific J. Trop. Biomed. J. Homepage. (2011) S55–S57.

[99] X. Pascoal, D. Teresa, L. Dias, The Role of Honey and Propolis in the Treatment of Infected Wounds. Microbiology for Surgical Infections, Well Helman Press, London, 2014.

Figure captions:

Fig 1. HPLC chromatograms of chrysin (A) and propolis extract (B).

Fig. 2 Mean diameters (ZAverage) and polydispersity index (PdI) of: solid lipid nanoparticles SLN (A and B); nanostructured lipid carriers NLC (C and D). The results correspond to three determinations on different batches of the same dispersion, standard deviation was always comprised between ± 5%.

Fig. 3 Cryo-transmission electron microscopy images (cryo-TEM) of: (A) NLC-B, (B) SLN-B, (C) NLC-2, (D) SLN-2, (E) NLC-4 and (F) SLN-4. The inserts show in more detail the shape of the SLN and NLC.

Fig. 4. X-ray diffraction profiles obtained from: (A) tristearin; (B) propolis extract (PE); (C) poloxamer; (D) propolis byproduct extract (BPE).

Fig. 5. X-ray diffraction profiles obtained from physical mixture of blank nanoparticles (PM-B) and of the nanoparticles loaded with PE (PM-PE) and BPE (PM-BPE). Besides the SLN-B, NLC-B, SLN-2, NLC-2; SLN-4 and NLC-4.

Fig. 6. *In vitro* release profile of polyphenols from the free drugs (propolis extract – PE and byproduct extract – BPE) and from the nanoparticles: (A) PE (♦), SLN-2 (●) and NLC-2 (▲); (B) BPE (●), SLN-4 (■) and NLC-4 (♦). Each curve is the mean ± standard deviation of at least three analyses.

Fig. 7 Occlusion factor of blank lipid nanoparticles (SLN-B and NLC-B); lipid nanoparticles loaded with propolis extract (SLN-2 and NLC-2) and lipid nanoparticles loaded with byproduct extract (SLN-4 and NLC-4) as a function of time.

Fig. 8. Cell viability of human immortalized keratinocytes (HaCaT): (a) SLN-B; (b) SLN-4; (c) propolis extract (PE), propolis byproduct extract (BPE) and ethanol 70% (w/w), where A, B, C e D, correspond to the concentrations of 3, 6, 30 and 60 μL for PE and ethanol and 4, 8, 40 e 80 μL for the BPE.

Fig. 9. Representative photographs showing the wounds and the different treatments in SKH1- mice: after treatment (d0); after 15 days of treatment (d15).

Fig.10. The results for the quantification of wound closure in terms of percentage of original wound size and in function of time (days)

Table 1

Composition of solid lipid nanoparticles (SLN) and nanostructured lipid carriers (NLC) compositions

Formulation	Composition (%, w/w)				
	P188d	Tristearin	Tricaprin	PE	BPE
SLN-B	95	5	-	-	-
SLN-1	95	5	-	0.1	-
SLN-2	95	5	-	1.4	-
SLN-3	95	5	-	-	0.1
SLN-4	95	5	-	-	0.8
NLC-B	95	3.35	1.65	-	-
NLC-1	95	3.35	1.65	0.1	-
NLC-2	95	3.35	1.65	1.4	-
NLC-3	95	3.35	1.65	-	0.1
NLC-4	95	3.35	1.65	-	0.8

P188d: Poloxamer 188 aqueous dispersion 2.5%, w/w; PE or BPE were added to the formulation in relation to DR%.

Table 2

Results of physicochemical analysis of the quality control of: propolis (PE) and byproduct extract (BPE).

Analysis	PE	BPE
pH	5.12 ± 0.05	5.89 ± 0.01
Density (g/mL)	0.87 ± 0.00	0.85 ± 0.00
Dryness residue (%,w/w)	19.33 ± 0.01	11.19 ± 0.40
Alcoholic content (%, w/w)	67.33 ± 2.20	53.86 ± 1.97
Total phenol content (%, w/V)	1.42 ± 0.07	0.30 ± 0.06

All values are represented by the average of at least three repetitions (± standard deviation).

Table 3

Statistical data (accuracy, precision, and robustness) of the validation of HPLC method for propolis analysis and the entrapment efficiency of nanostructured lipid systems (SLN and NLC) containing propolis extract or propolis byproduct extract.

Chrysin (μg/mL)	Accuracy					
	Chrysin (μg/mL)		Recovery (%)		Mean Recovery (%)	
50.00	49.55 ± 0.07		99.10 ± 0.13			
6.25	6.12 ± 0.02		97.86 ± 0.26		98.95 ± 1.05	
1.56	1.57 ± 0.02		99.88 ± 1.12			
	Precision					
	Repeatability		Intermediate Precision			
	Intra-day (μg/mL)	RSD (%)	Inter-day (μg/mL)	RSD (%)	Precision (analyst 2) (μg/mL)	RSD (%)
50.00	49.70 ± 0.25	0.49	49.81 ± 0.37	0.74	49.55 ± 0.06	0.13
6.25	6.07 ± 0.03	0.49	6.12 ± 0.09	1.56	6.12 ± 0.02	0.26
1.56	1.56 ± 0.01	0.59	1.56 ± 0.02	1.34	1.56 ± 0.02	1.12
	Robustness (μg/mL)					
	Wave-length (nm)/ flow (mL/min)					
	290/1.0		310/0.8		310/1.0	
50.00	48.70		49.76		49.70	
6.25	6.03		6.26		6.13	
1.56	1.55		1.53		1.54	
Sample	Entrapment efficiency (%)					
SLN-2	40.19 ± 0.31					
NLC-2	31.93 ± 1.01					
SLN-4	60.58 ± 1.17					
NLC-4	81.94 ± 1.28					

Table 4

Release kinetic parameters for the chrysin release from solid lipid nanoparticles (SLN-2 and SLN-4), nanostructured lipid carriers (NLC-2 and NLC-4), propolis extract (PE), and propolis byproduct extract (BPE).

Sample	Kinetic release parameters		
	n	K (h^{-1})	R^2
PE	0.61	1.18	0.85
BPE	0.66	12.22	0.79
SLN-2	0.45	0.34	0.95
NLC-2	0.46	0.78	0.88
SLN-4	0.48	2.24	0.99
NLC-4	0.45	2.50	0.97

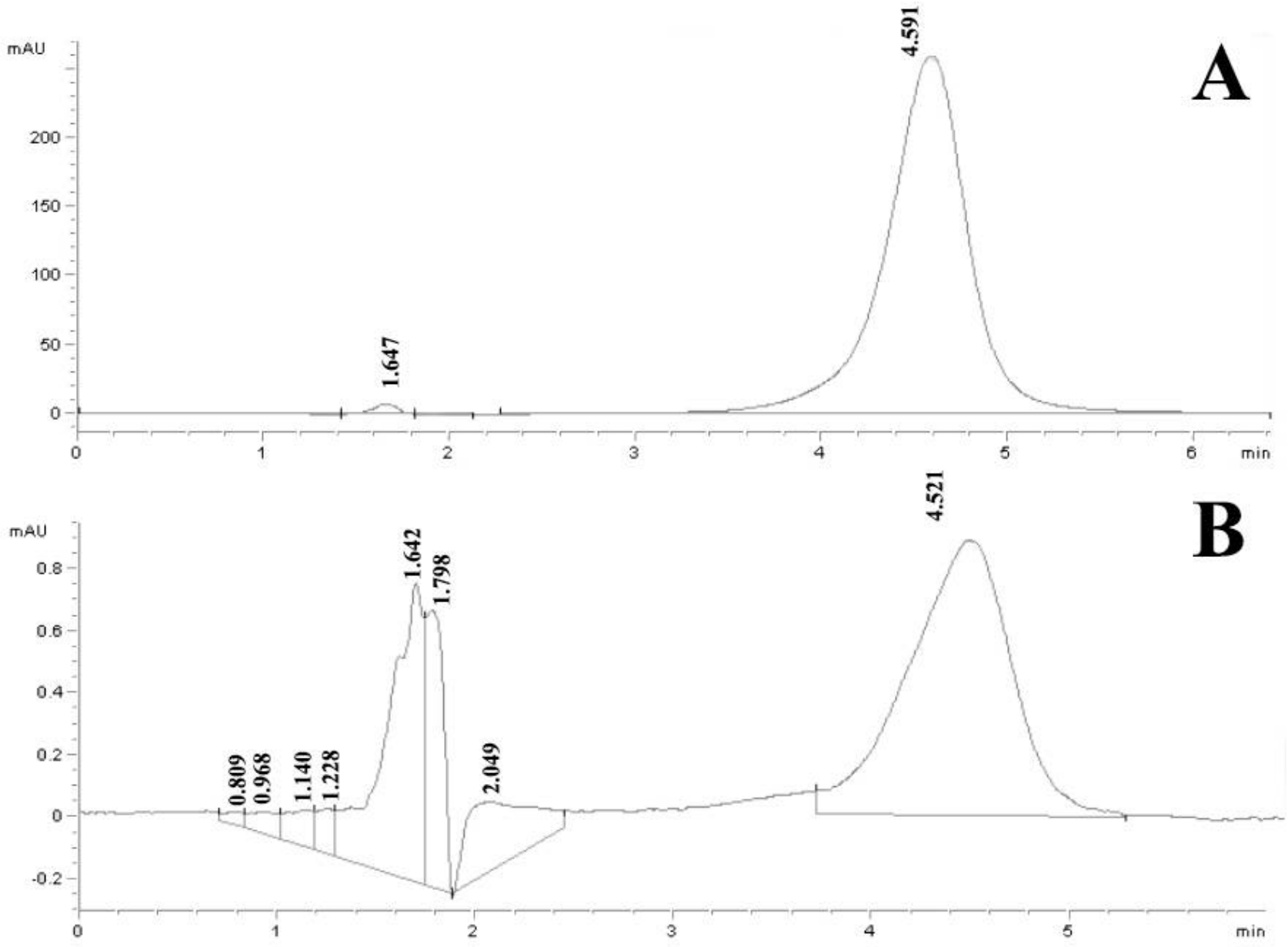
A
mAU
200
150
100
50
0
1.647
4.591
0
1
2
3
4
5
6
min
B
mAU
0.8
0.6
0.4
0.2
0
-0.2
0.809
0.968
1.140
1.228
1.642
1.798
2.049
4.521
0
1
2
3
4
5
min

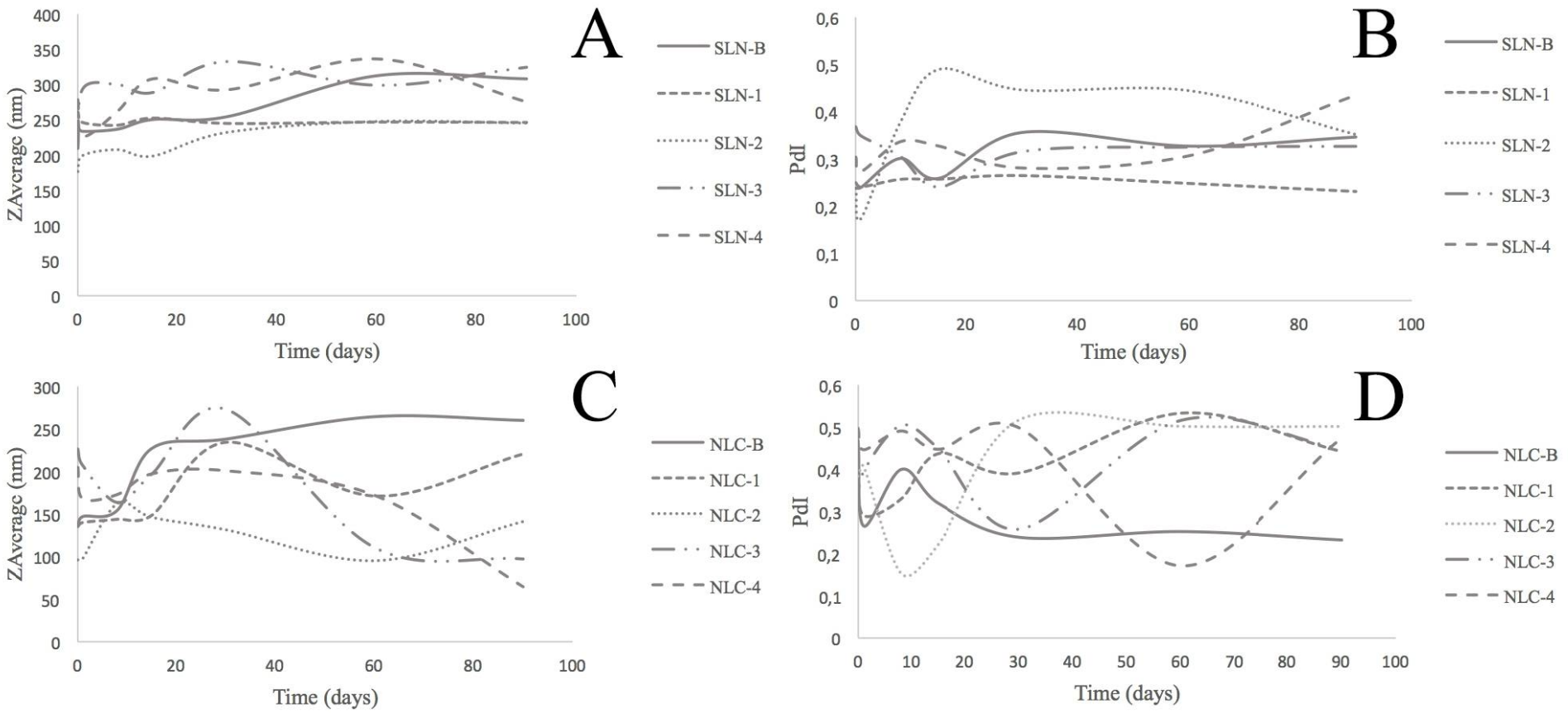
A
ZAvcragc (nm)
400
350
300
250
200
150
100
50
0
0
20
40
60
80
100
Time (days)
SLN-B
SLN-1
SLN-2
SLN-3
SLN-4
B
PdI
0,6
0,5
0,4
0,3
0,2
0,1
0
0
20
40
60
80
100
Time (days)
SLN-B
SLN-1
SLN-2
SLN-3
SLN-4
C
ZAvcragc (nm)
300
250
200
150
100
50
0
0
20
40
60
80
100
Time (days)
NLC-B
NLC-1
NLC-2
NLC-3
NLC-4
D
PdI
0,6
0,5
0,4
0,3
0,2
0,1
0
0
10
20
30
40
50
60
70
80
90
100
Time (days)
NLC-B
NLC-1
NLC-2
NLC-3
NLC-4

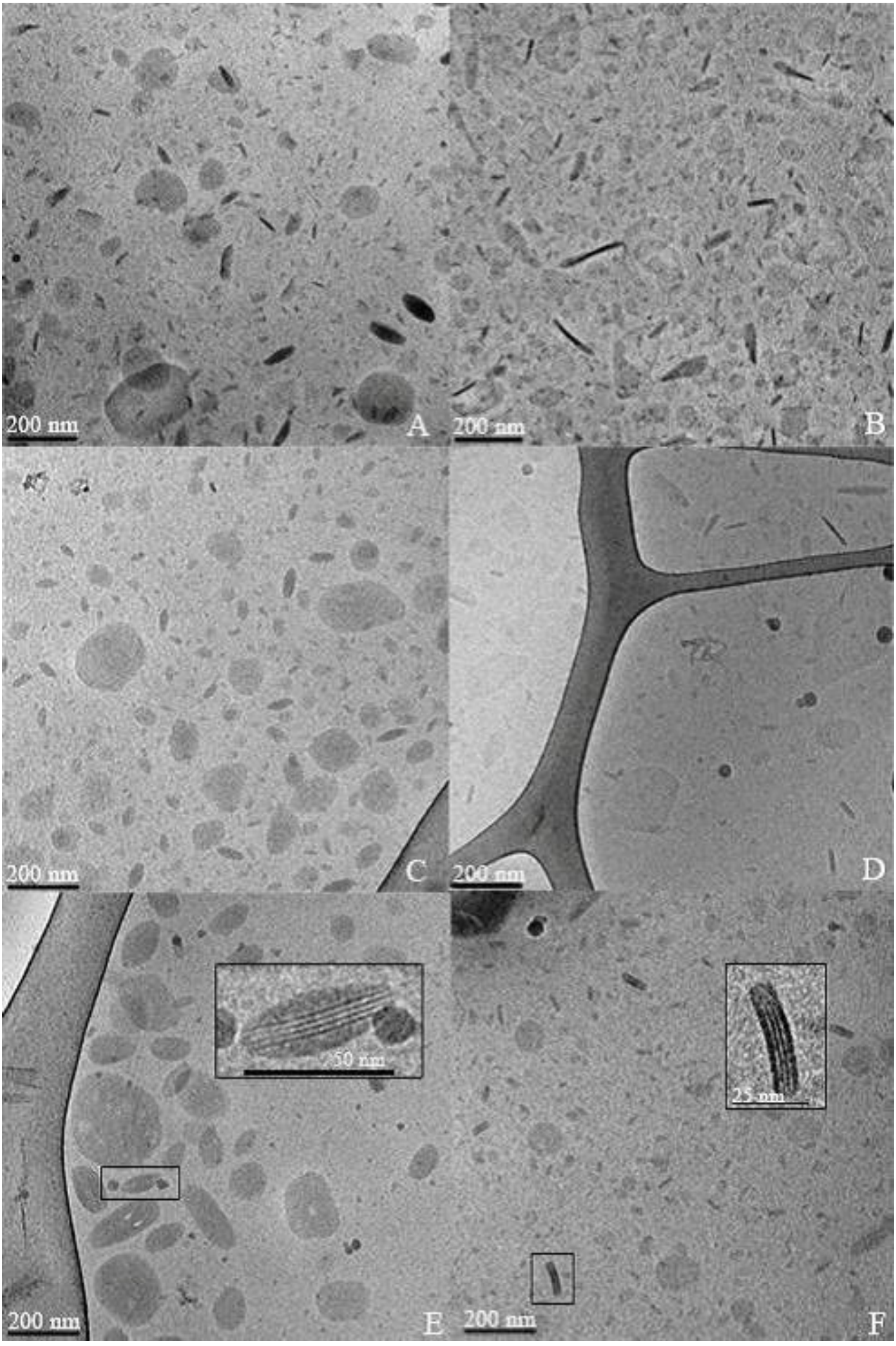
200 nm
A
200 nm
B
200 nm
C
200 nm
D
50 nm
25 nm
200 nm
E
200 nm
F

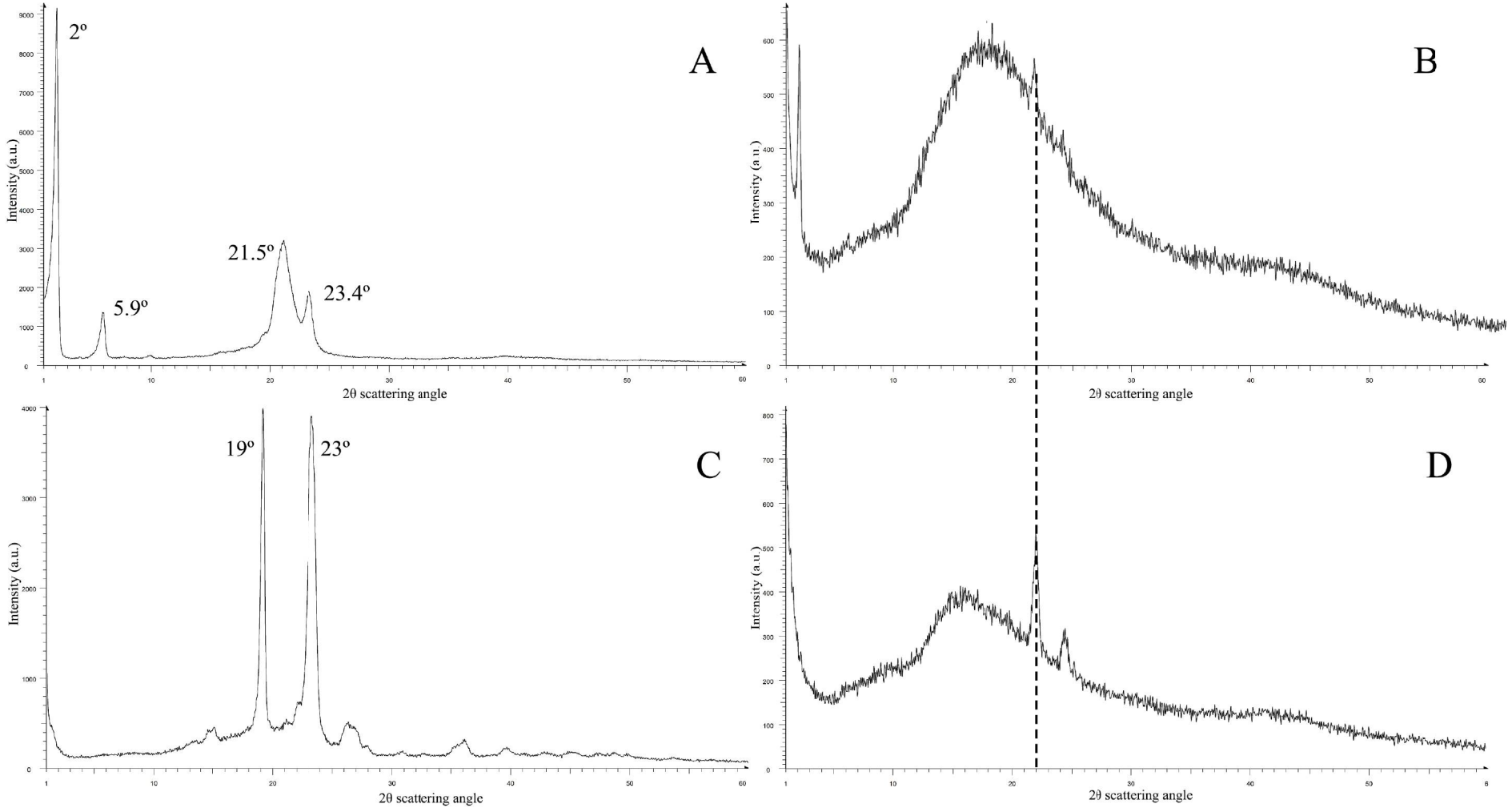
A
2º
5.9º
21.5º
23.4º
Intensity (a.u.)
2θ scattering angle
B
Intensity (a.u.)
2θ scattering angle
C
19º
23º
Intensity (a.u.)
2θ scattering angle
D
Intensity (a.u.)
2θ scattering angle

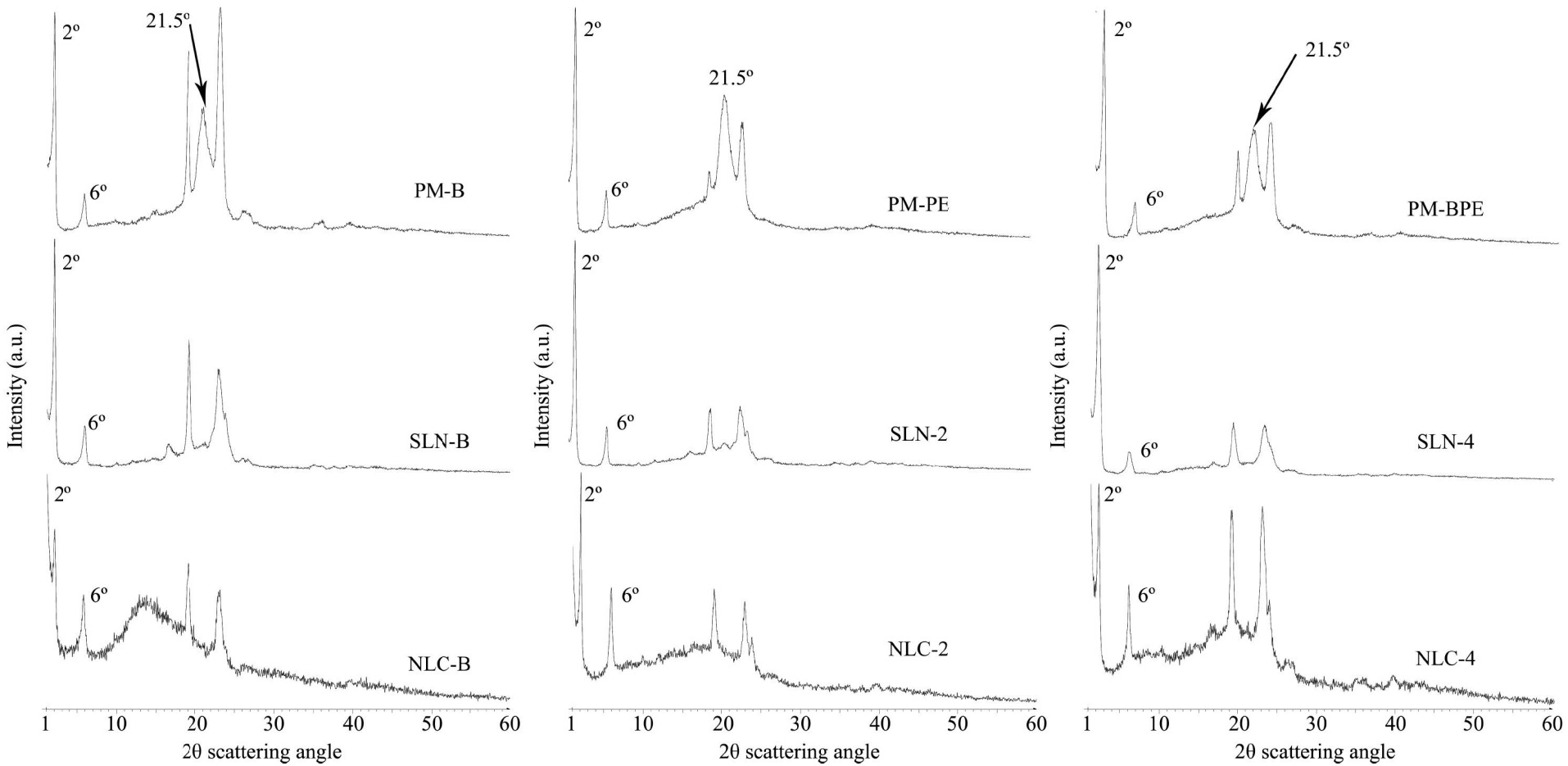
2º
21.5º
6º
PM-B
SLN-B
NLC-B
PM-PE
SLN-2
NLC-2
PM-BPE
SLN-4
NLC-4
Intensity (a.u.)
1
10
20
30
40
50
60
2θ scattering angle

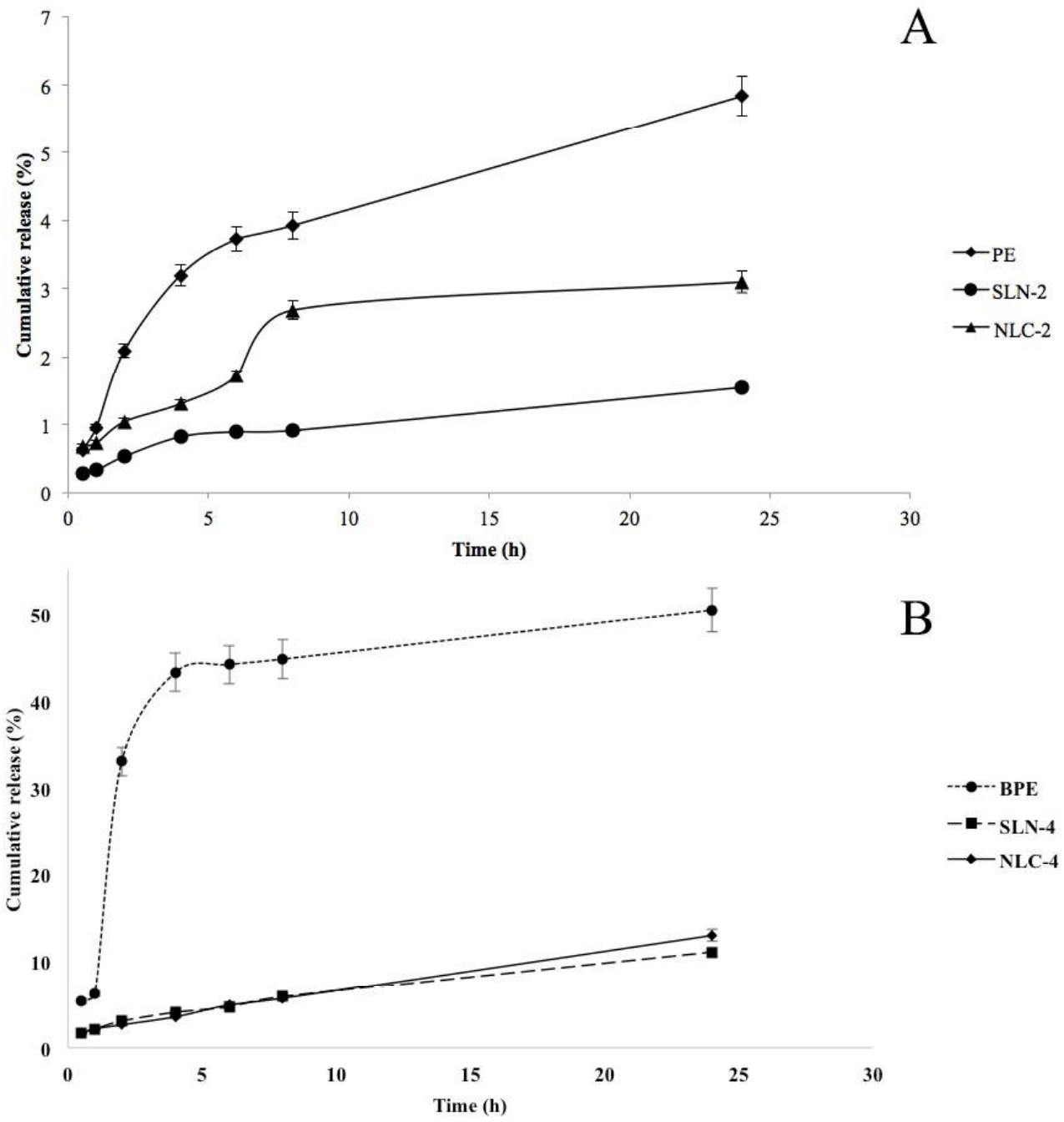
A
Cumulative release (%)
Time (h)
PE
SLN-2
NLC-2
B
Cumulative release (%)
Time (h)
BPE
SLN-4
NLC-4

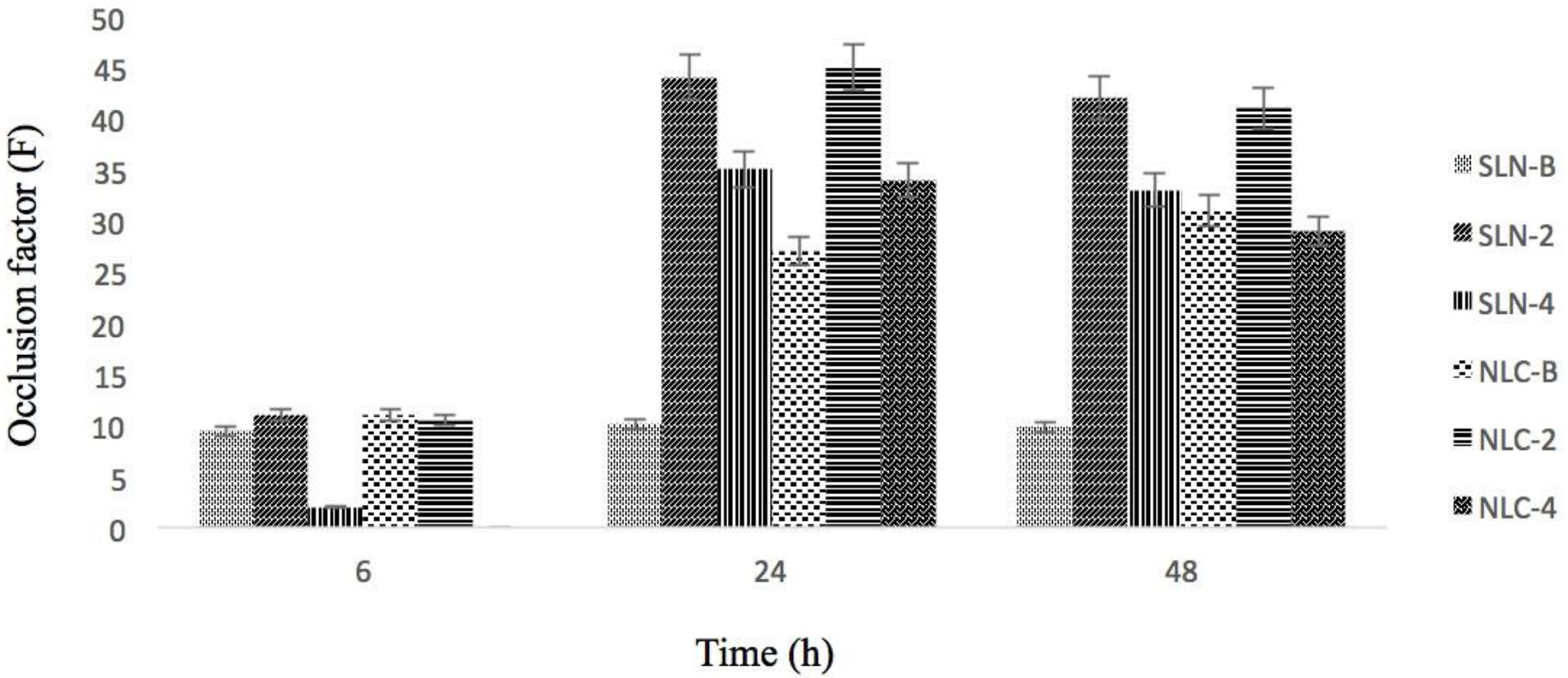
50
45
40
35
30
25
20
15
10
5
0
Occlusion factor (F)
6
24
48
Time (h)
SLN-B
SLN-2
SLN-4
NLC-B
NLC-2
NLC-4

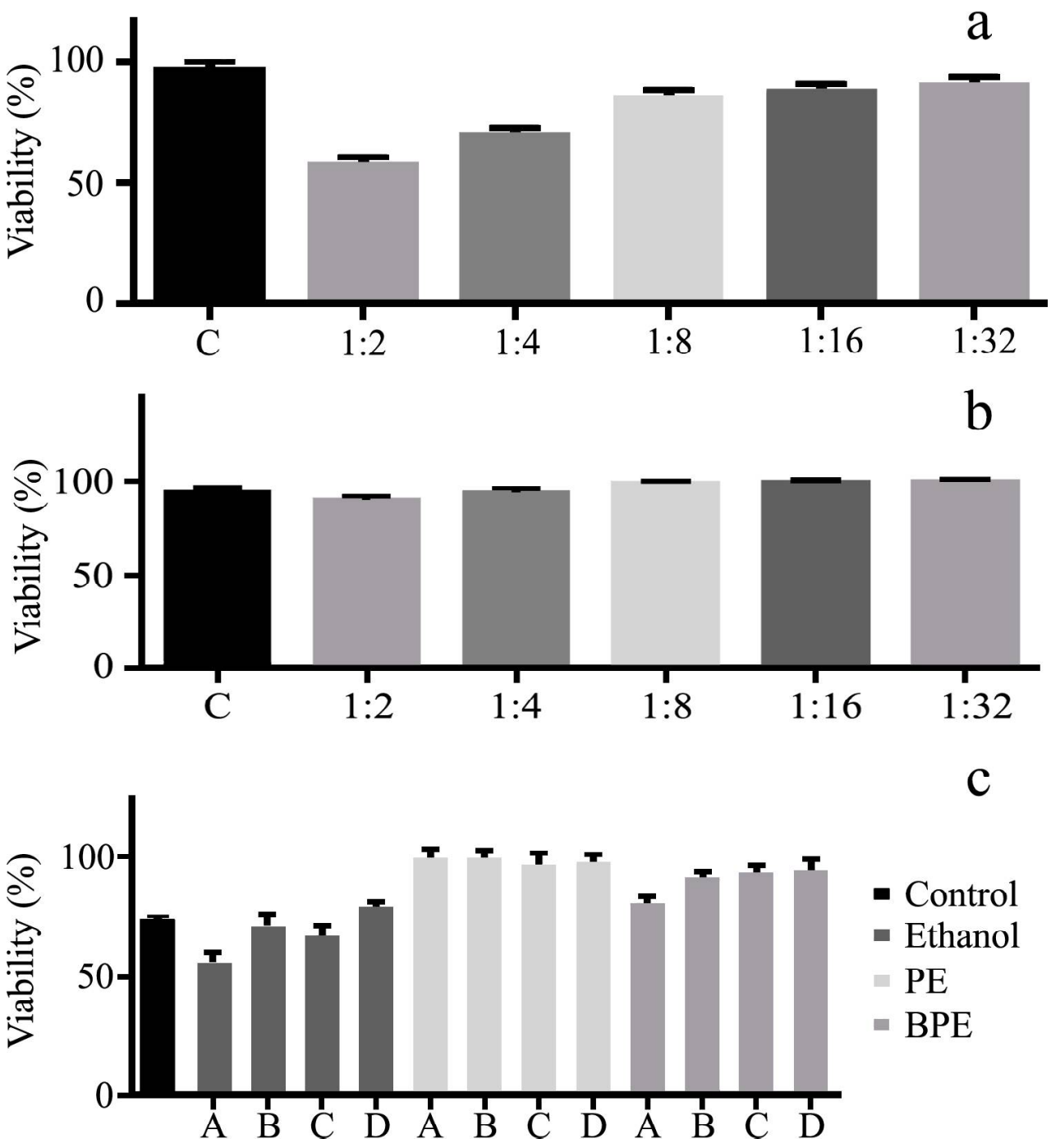
a
Viability (%)
100
50
0
C
1:2
1:4
1:8
1:16
1:32
b
Viability (%)
100
50
0
C
1:2
1:4
1:8
1:16
1:32
c
Viability (%)
100
50
0
A B C D A B C D A B C D
Control
Ethanol
PE
BPE

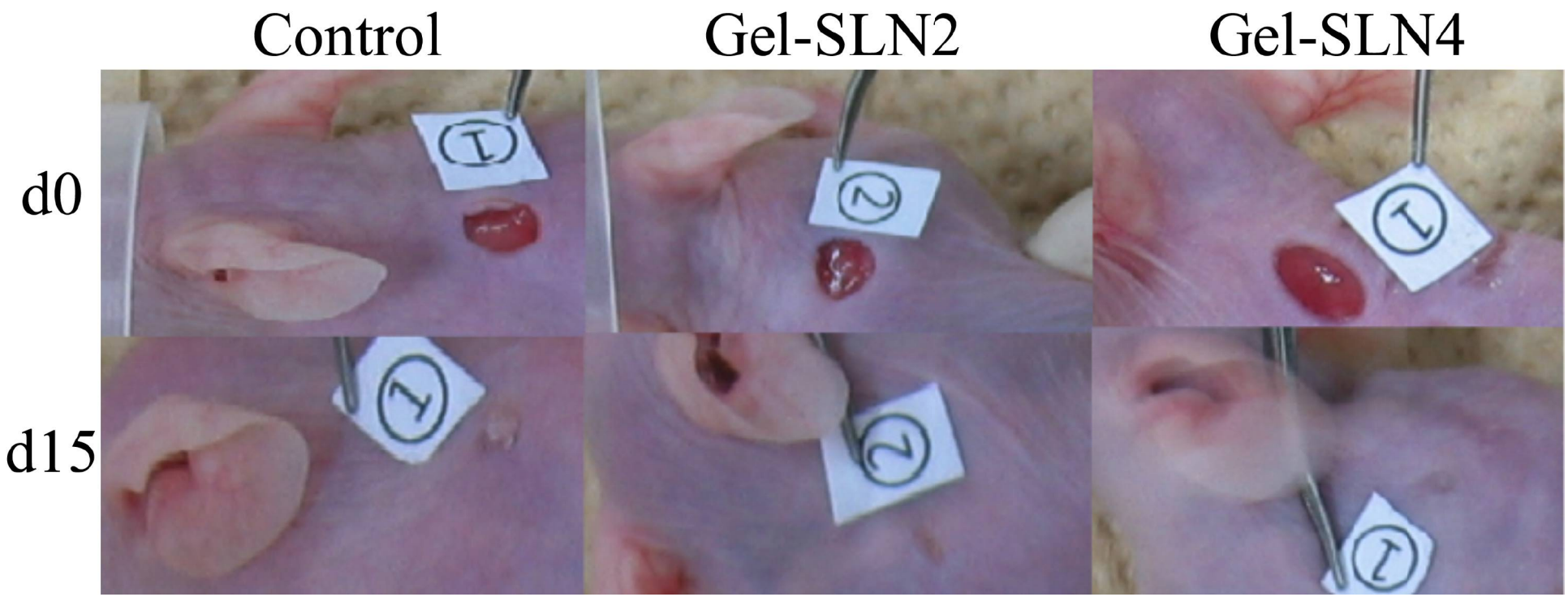
Control
Gel-SLN2
Gel-SLN4
d0
d15

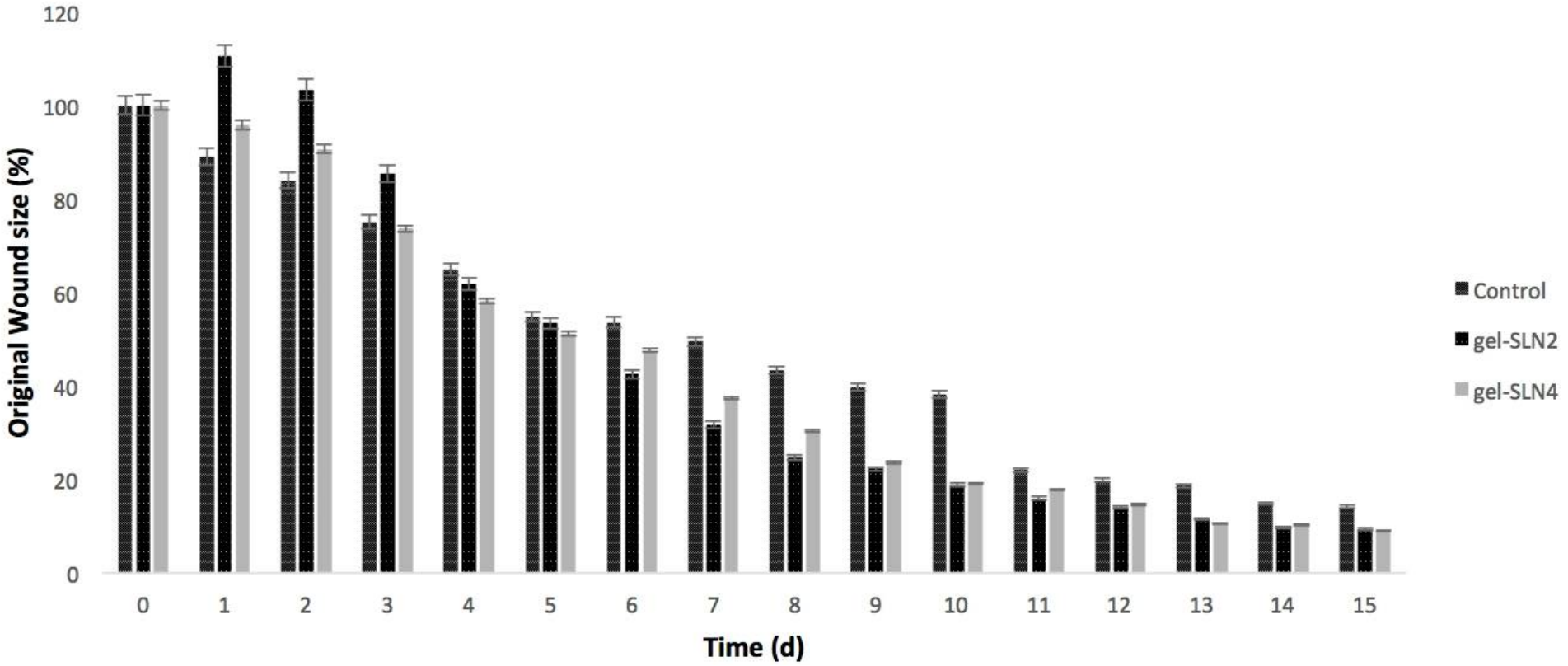
120
100
80
60
40
20
0
Original Wound size (%)
0
1
2
3
4
5
6
7
8
9
10
11
12
13
14
15
Time (d)
Control
gel-SLN2
gel-SLN4

Highlights

- The development of nanostructured lipid systems containing propolis or its waste material is proposed.
- The propolis and waste material extracts displayed good physicochemical characteristics.
- Lipid systems were characterized as morphology, size analysis, and diffractometric (X-ray) characteristics.
- The occlusive capacity of the formulations, entrapment efficiency, and the *in vitro* drug release profile enabled to select the best formulations.
- The systems display no cell toxicity and acceleration of the wound healing process tested *in vivo*.